2014

The Composition and Downward Vertical Transport of Particulate Phosphorus in the Cariaco Basin, Venezuela

Anne S. Opseth
University of South Carolina - Columbia

THE COMPOSITION AND DOWNWARD VERTICAL TRANSPORT OF PARTICULATE PHOSPHORUS IN THE CARIACO BASIN, VENEZUELA

by

Annie S. Opseth

Bachelor of Arts
Gustavus Adolphus College, 2010

Submitted in Partial Fulfillment of the Requirements

For the Degree of Master of Science in

Marine Science

College of Arts and Sciences

University of South Carolina

2014

Accepted by:

Claudia Benitez-Nelson, Director of Thesis

Robert Thunell, Reader

Tammi Richardson, Reader

Lacy Ford, Vice Provost and Dean of Graduate Studies

ACKNOWLEDGEMENTS

The completion of this thesis would not have been possible without the help and support from many people, both professionally and personally. My research experiences and interactions with wonderful people have made my years at the University of South Carolina memorable and enjoyable.

I must begin with thanking my advisor, Dr. Claudia Benitez-Nelson. It is because of her guidance, encouragement and support that I have come so far in my education and career. Her enthusiasm and drive are infectious and her constant support through the entire process is the primary reason I've come so far. My gratitude for her is infinite.

Another person that has helped me tremendously is our lab manager, Wendy Plessinger. Her help and feedback with experiments, data and writing has been invaluable during my time here at USC. I could always count on her to help me with any problems or questions pertaining to my research and for this I am very grateful.

A huge thank you must also be extended to Perry Pellechia, USC's NMR guru, who helped me run countless samples and interpret spectra and to Eric Tappa who led me in my amazing research cruise experiences and helped me with all things Cariaco.

Finally I must acknowledge the extreme value in having the support and camaraderie of my fellow grad students, especially my lab mates, Sharmila Pal, Meryssa Downer, Doug Bell, Erin McParland and Melissa Bennett. And of course, I couldn't have done this without the huge amount of love and support I received from my family and friends.

ABSTRACT

In order to understand the biogeochemical cycling of phosphorus (P) in a coastal marine ecosystem, the chemical composition and the sinking flux of particulate P was analyzed within sediment trap particles collected in the Cariaco Basin, Venezuela. Total, inorganic and organic P composition was examined across the time series (1995-2010) using a modified Aspila method and sequential extraction techniques. Particulate inorganic P (PIP) dominated the total particulate P (TPP) pool (~52%) when averaged over the entire water column. Relationships between particulate nitrogen (PN) and particulate organic carbon (POC) fluxes versus TPP fluxes followed expected canonical Redfield ratios except for a series of samples that were comprised with extraordinarily high fluxes of PIP. This suggests that a significant fraction of PIP is marine derived, with the high PIP flux events likely due to coastal margin and terrigenous inputs. PIP composition in both high and low flux events associated with Redfield and non-Redfield particulate nutrient ratios were examined in detail using SEDEX, a sequential chemical extraction method that focuses on inorganic P associations. Results indicate that most of the "extra" PIP is in the form of labile and oxide bound P, suggesting that it is likely to be bioavailable to marine organisms on relatively short timescales. Indeed, a significant fraction of this "high" PIP was rapidly remineralized with increasing depth. Low terrigenous fluxes and a lack of strong detrital or authigenic P source suggest that the higher PIP fluxes are likely due to remobilization of marine organic matter of lithogenic origin from the Unare platform.

Techniques were also tested for examining specific compounds within sediment trap material using the Miyata & Hattori (M&H) sequential extraction method. The M&H method was optimized using known P compounds as spikes and combining the extraction with solid and liquid state ^{31}P-NMR. Specifically we were able to verify the presence of two P compounds that were spiked and extracted using M&H via ^{31}P-NMR, DNA and sodium hexametaphosphate. A limited number of sediment trap samples were analyzed using the M&H method and our results suggest that > 50% of the P present in the samples are comprised of nucleotides, sugar phosphates and orthophosphate, followed by lipids, polyphosphates and nucleic acids, compounds previously observed in sediments. In contrast, Miyata & Hattori (1986) found orthophosphate and nucleic acids to be the most abundant types of P in phytoplankton, followed by polyphosphates and lipids.

The biogeochemical cycling of P is complicated and various factors need to be considered, for example remineralization and sources (terrestrial, biological, etc.). However, the use of SEDEX, M&H and ^{31}P-NMR, together and individually, help us better understand the behavior and composition of this important nutrient.

TABLE OF CONTENTS

LIST OF TABLES

LIST OF FIGURES

CHAPTER 1: INTRODUCTION

1.1 Background

Phosphorus (P) is an important macronutrient in marine and lacustrine ecosystems (Froelich et al., 1982; Benitez-Nelson, 2000; Karl and Björkman, 2002; Paytan and McLaughlin, 2007; Martiny et al., 2013). Similar to carbon (C) and nitrogen (N), P plays a role in a variety of biologically important processes including photosynthesis, respiration, energy transport and storage (Froelich et al., 1982; Paytan and McLaughlin, 2007). As a result, many surface waters of the world's oceans are regularly P-stressed (Karl et al., 2008; Hannides et al., 2009). Yet, P remains relatively under studied compared to other biologically important elements, such as C and N, and even trace elements, such as iron. As recently as 2011, there are three times as many publications focusing on marine N as there are on marine P (Figure 1.1).

P is primarily delivered in particulate form to the coastal oceans by riverine transport (~90% of the total P pool) as a result of continental weathering and runoff (Delaney, 1998; Benitez-Nelson, 2000; Paytan and McLaughlin, 2007; Sekula-Wood et al., 2012). A large percentage (~70%) of this riverine P is directly deposited on the continental shelves and essentially removed from the P cycle over geologic timescales (Benitez-Nelson, 2000; Paytan and McLaughlin, 2007; Sekula-Wood et al., 2012). The remaining P undergoes a number of major transformations within the water column, most of which are biologically driven, e.g., during carbon fixation and remineralization (Figure 1.2).

Phytoplankton have the ability to break down a wide range of dissolved and particulate P compounds into phosphate via enzymatic reactions that hydrolyze orthophosphate from organically-bound P (Karl and Björkman, 2002; Dyhrman et al., 2006, 2009; White et al., 2010). Plankton acquisition of phosphate, often used interchangeably with dissolved inorganic P (DIP), involves the use of ATP to actively transport P across their cell membranes (Dyhrman et al., 2007; White et al., 2010). When DIP concentrations are too low for them to maintain their biological demands, a wide variety of alternative enzymatic pathways are activated to utilize dissolved organic P (DOP), although some phytoplankton may use DOP even when DIP concentrations are significant (> 0.2 μM P) (Ranhofer et al., 2009). DOP includes such compounds as: nucleic acids, nucleotides, phospholipids, sugar phosphates and even phosphonates, which all require enzymatic reactions to cleave phosphate from the rest of the molecule (White et al., 2010; Young and Ingall, 2010). For example, marine microorganisms may access DIP using phosphatase, an enzyme capable of breaking P monoesters, or nucleotidase, an enzyme that breaks down nucleic acids (Ammerman and Azam, 1985, 1991a, 1991b). Until recently, phosphonates were thought to be inaccessible to marine microorganisms, yet it is now recognized that phosphonates may be accessed by the use of an enzyme, C-P lysase, which has the ability to break down sturdy C-P bonds (Dyhrman et al., 2006; Karl et al., 2008; White et al., 2010). Such degradation has implications far beyond the P cycle. For example, cyanobacteria may break down and use methylphosphonates, which contain strong C-P bonds that are generally resistant to abiotic decomposition, resulting in the production and release of the greenhouse gas methane in P-stressed waters (Karl et al., 2008).

Within marine plankton, phospholipids, DNA and ATP are key P-containing cellular and structural components (Benitez-Nelson, 2000; Sannigrahi et al., 2006; Paytan and McLaughlin, 2007; Lomas et al., 2010). Molar ratios of C:P and N:P are highly variable within these organisms suggesting a diversity in biochemical composition within the taxon (Hannides et al., 2009; Martiny et al., 2013). Yet, there is relatively little information regarding the composition and flux of particulate P to depth and how this flux changes seasonally and under different environmental conditions, such as oxygen content and acidity (Benitez-Nelson et al., 2007; Lyons et al., 2011; Sekula-Wood et al., 2012). A variety of compounds are released in both particulate and dissolved forms into the surrounding water column via cell death and lysis, sloppy feeding, zooplankton repackaging, etc. (Lampert, 1978; Longhurst, 1991; Wilson et al., 2008). Most research has focused on the relative composition of the total particulate phosphorus (TPP) pool, with little differentiation between inorganic and organic components.

1.2 Marine Particulate Phosphorus (PP) speciation

1.2.1 P sources and distribution

The major source of PP to the coastal ocean is riverine input, although it can also be introduced into the oceans by IRD (ice-rafted debris) and eolian dust (Ruttenberg, 2003; Paytan and McLaughlin, 2007; Wallmann, 2010). Near the river mouth a significant portion of riverine-sourced PP is removed via sedimentation (Delaney, 1998; Sekula-Wood et al., 2012). This is due to coastal waters receiving large riverine inputs and their shallower depths, resulting in increased burial of PP in sediments (Ruttenberg, 2003). A large portion of the marine PP that is not removed, and deposited on the continental margin seafloor, is released into the dissolved phase (Froelich et al., 1982;

Delaney, 1998; Ruttenberg 2003; Wallmann, 2010). This is due to the deeper water column and subsequently, longer remineralization time. Indeed, very little of the PP produced in the open ocean is buried upon reaching the ocean floor (Ruttenberg, 2003).

Within the water column, PP can be suspended or sinking entities depending on particle density. PP concentrations in the water column have an inverse relationship with depth, with high concentrations in surface waters and low concentrations deeper in the water column, reflecting the importance of phytoplankton as a PP source (Hebel and Karl, 2001; Suzumura and Ingall, 2004; Faul et al., 2005) and the rapid remineralization of P within the water column (Benitez-Nelson et al., 2004). Fine or non-aggregated particles remain suspended for variable lengths of time before slowly reaching the ocean floor, if ever (Faul et al., 2005; Paytan and McLaughlin, 2007). Sinking PP is formed via sloppy feeding, aggregation of these fine particles, and fecal pellets. Those with higher densities sink more rapidly, on the order of days to weeks (Lampert, 1978; Longhurst, 1991; Clark et al., 1999; Paytan et al., 2003; Wilson et al., 2008).

While sinking PP varies significantly with season, suspended PP distributions are relatively invariant (Faul et al., 2005). For example, Hebel and Karl (2001) observed that PP concentrations at Station ALOHA within in the euphotic zone (EZ) of the North Pacific Subtropical Gyre (NPSG) showed only a slight seasonal variation, except for an apparent winter minimum. The opposite trend was observed for sinking PP, particulate carbon (PC), and particulate nitrogen (PN), all exhibiting summer/fall maxima.

Long term trends have only recently begun to be examined due to the paucity of data available, but we do have some initial studies looking at long term trends that have just recently been published. Lomas et al. (2013) found that over the 24 years of data

collection at the Bermuda Atlantic Time-series Study (BATS), the particulate P:N ratio in sediment traps has decreased from 50-75 to < 50, indicating a decrease in PN or increase in PP; they believe this decrease in the P:N ratio may be due to increased nitrogen remineralization. They have also found that PP fluxes have increased significantly at all sediment trap depths, which could be due to changes in the remineralization rates of N or P, although it is more likely N is being recycled faster and there's been a change in the plankton community thus altering the source of sinking particulate organic matter. At Station ALOHA, the site of the Hawaii Ocean Time-series (HOT) research program, the export rate of P from the surface ocean has decreased over the course of the time series (1988-Present) while C and N have not (Karl, 2014). At the beginning of the time series, molar C:N:P ratios were closer to the canonical Redfield; however, as of 2011, C:N:P ratios are as high as 186:28:1, reflecting the depletion in P relative to C and N.

1.2.2 P composition

PP is comprised of a wide range of compounds that vary in their biological and chemical reactivity. As such, PP composition can vary greatly from area to area. Martiny et al. (2013) found that there are substantial latitudinal variations in upper ocean plankton elemental ratios from the widely accepted Redfield ratio of 106C:16N:1P (Redfield, 1958). They observed a clear trend of high N:P ratios in warm, nutrient-depleted waters at the equator dominated by the cyanobacteria *Prochlorococcus* and *Synechoccus*, picoeukaryotes and the heterotrophic bacterium Pelagibacter, with these ratios decreasing in to colder, nutrient-rich waters at higher latitudes dominated by diatoms and large eukaryotes. They suggested that this change was due to temperature, nutrient concentrations and variability in plankton assemblages.

Despite PP's biological origins at the surface (~80% POP), a major component (20-40%) of sinking PP is in its inorganic form, PIP, and is the primary mechanism for delivering reactive P to marine sediments (Delaney, 1998; Paytan et al., 2003; Paytan and McLaughlin, 2007; Yoshimura et al., 2007; Lyons et al., 2011; Sekula-Wood, 2012). In coastal environments, a large component of the PIP is derived from terrestrial sources, e.g. continental weathering via riverine input and the relative percentage of PIP can exceed 80% (Ruttenberg, 2003; Paytan and McLaughlin, 2007; Sekula-Wood et al., 2012).

Contrary to the conclusion of past studies that the majority of sinking TPP is composed of POP (Benitez-Nelson, 2000; Lyons et al., 2011), more recent studies have shown that a significant portion is in fact PIP (Paytan et al., 2003; Benitez-Nelson et al., 2007; Lyons et al., 2011). PIP can be categorized into four fractions: loosely bound or labile, oxide-associated, authigenic and detrital. Earlier studies of marine sinking PP assumed that it is mostly composed of organic P; however, recent studies have found PIP to comprise a significant portion of TPP in coastal regions (Lyons et al., 2011). Some examples of PIP comprising a larger portion of TPP are in the Gulf of California (69±15%), the Cariaco Basin (52±19%) and the Santa Barbara Basin (85±5%), where PIP is preferentially remineralized over POP in anoxic waters, likely due to oxide reduction (Benitez-Nelson et al., 2007; Lyons et al., 2011). The same trend can be seen in the open ocean. Loh and Bauer (2000) found PIP to comprise up to 80% of the TPP pool in suspended and sinking particulate organic matter (POM) in the eastern North Pacific and Southern oceans.

P esters (Kolowith et al., 2001; Clark et al., 1999) and phosphonates (Benitez-Nelson et al., 2004) are the primary P compound classes measured in POP. In anoxic waters, the percentage of phosphonate present in the TPP pool decreases with depth relative to P esters; this suggests that phosphonates are being preferentially remineralized over more biologically available P compounds (Benitez-Nelson et al., 2004) and is a potential source for dissolved inorganic P (DIP) under these conditions (Paytan and McLaughlin, 2007). Dyhrman et al. (2009) identified the phosphonate bond (P-C) in cultures of the cyanobacteria, *Trichodesmium erythraeum*. Upon increasing the TPP in the cultures, total phosphonate increased as well, indicating it is a function of TPP. In ultrafiltered particulate organic matter (UPOM) P is associated with amino acids, carbohydrates and lipids; the P associated with lipids is in the form of phospholipids which hold an important role in organisms' internal structures (Karl and Björkman, 2002; Sannigrahi et al., 2006). C:P and N:P average values of UPOM at Station Aloha are near Redfield, indicating a planktonic source (Sannigrahi et al., 2006).

In shallow waters, specifically the euphotic zone, POP dominates accounting for 80% of the TPP (Paytan and McLaughlin, 2007). However, as the TPP pool sinks deeper in the water column POP is being hydrolyzed and PIP becomes more dominant; at depth PIP makes up > 75% of the TPP pool (Paytan and McLaughlin, 2007). Relative to particulate organic carbon (POC), POP is rapidly remineralized in particles sinking throughout the oxic water column, and at a faster rate relative to POC and particulate organic nitrogen (PON) in oxic waters. Once POP enters anoxic waters, POC:PON:POP ratios remain relatively constant (Benitez-Nelson et al., 2007; Sekula-Wood et al., 2012).

This strong correlation between POP and POC reinforces that the source of sinking POP is biological (Sekula-Wood et al., 2012).

1.3 Conclusions

The above research suggests that focusing more attention on PP sources and composition will provide a more complete picture of the marine P cycle and its impact on marine biogeochemistry within present and over geological timescales (Benitez-Nelson, 2000; Yoshimura et al., 2007). The overarching goal of this thesis is to better understand the downward flux and composition of sinking PP material within the Cariaco Basin, Venezuela. Chapter 2 focuses on the bulk POP pool and examines PIP sources and compositional changes as material sinks across the oxic/anoxic boundary. Chapter 3 focuses on compositional changes within the POP pool using sequential extraction techniques and the development and application of liquid ^{31}P-NMR.

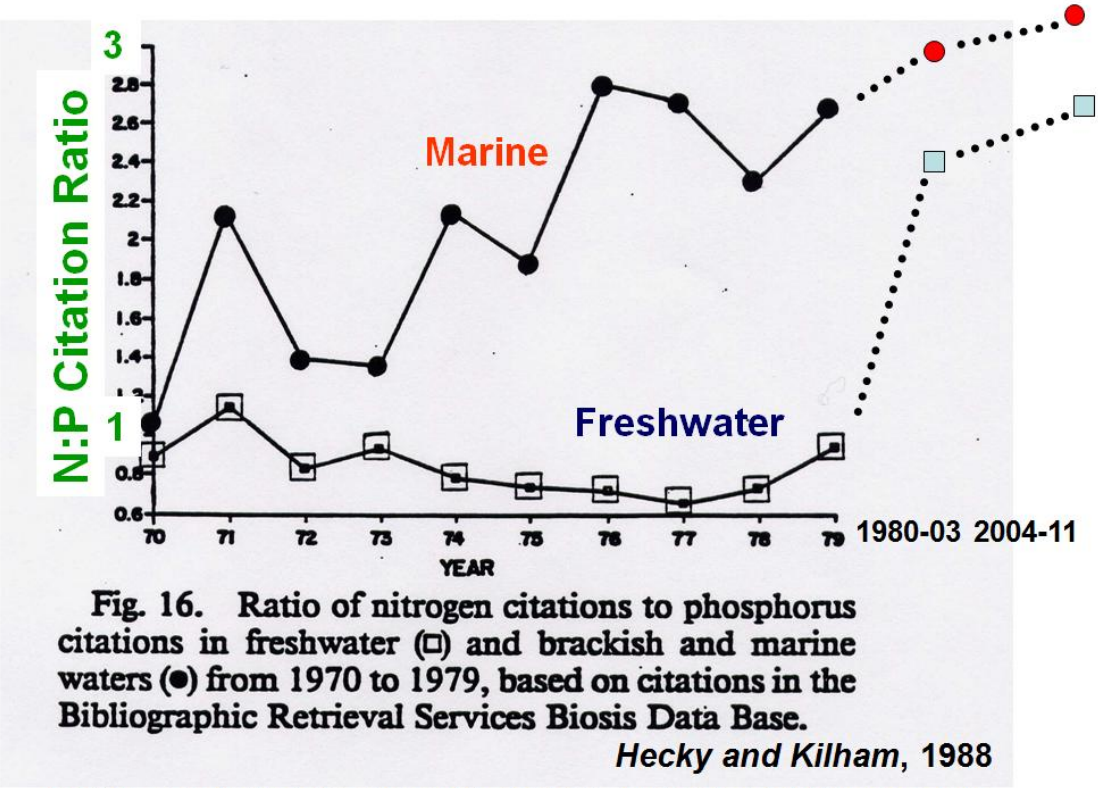

Fig. 16. Ratio of nitrogen citations to phosphorus citations in freshwater (□) and brackish and marine waters (●) from 1970 to 1979, based on citations in the Bibliographic Retrieval Services Biosis Data Base.

Hecky and Kilham, 1988

In 1970, equal numbers of N and P citations. By 1980, 3-fold increase in N versus P publications.

Figure 1.1 Ratio of N citations to P citations through 1980 (Hecky and Kilham, 1988) and then up through 2011 (Benitez-Nelson, 2012).

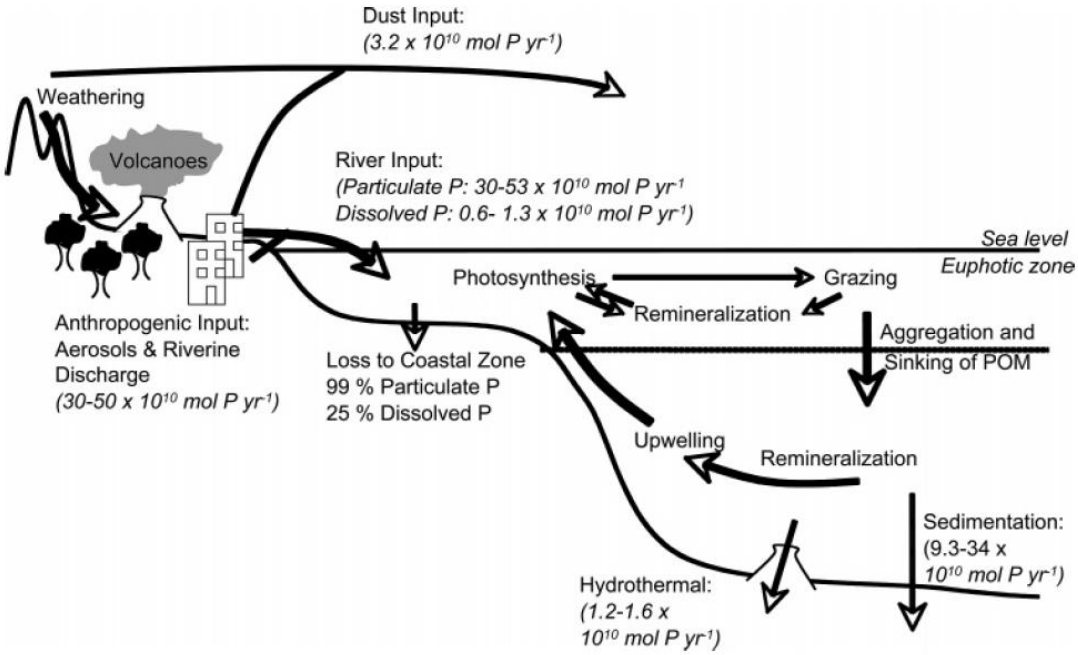

Figure 1.2 The marine phosphorus cycle (Paytan and McLaughlin, 2007).

CHAPTER 2: PARTICLUATE PHOSPHORUS COMPOSITION IN THE CARIACO BASIN, VENEZUELA

2.1 Introduction

Phosphorus (P) is an important macronutrient in marine and lacustrine ecosystems (Froelich et al., 1982; Benitez-Nelson, 2000; Karl and Björkman, 2002; Paytan and McLaughlin, 2007; Martiny et al., 2013). Similar to carbon (C) and nitrogen (N), P plays a role in a variety of biologically important processes including photosynthesis, respiration, energy transport and storage (Froelich, 1982; Paytan and McLaughlin, 2007). As a result, many of the world oceans are regularly P-stressed (Karl et al., 2008; Hannides et al., 2009). P is primarily delivered in particulate form to the coastal oceans by riverine transport (~90% of the total P pool) as a result of continental weathering and runoff (Delaney, 1998; Benitez-Nelson, 2000; Paytan and McLaughlin, 2007; Sekula-Wood et al., 2012). A large percentage (~70%) of this riverine P is directly deposited on the continental shelves and essentially removed from the P cycle over geologic timescales (Benitez-Nelson, 2000; Paytan and McLaughlin, 2007; Sekula-Wood et al., 2012). The remaining P undergoes a number of major transformations within the water column, most of which are biologically driven, e.g., during carbon fixation and remineralization.

Within the plankton, phospholipids, DNA and ATP are key P-containing cellular and structural components (Benitez-Nelson, 2000; Sannigrahi et al., 2006; Paytan and McLaughlin, 2007; Lomas et al., 2010). Molar ratios of C:P and N:P are highly variable within these organisms due to the wide variety of compounds that exist, suggesting a

diversity in biochemical composition within the taxon (Hannides et al., 2009; Martiny et al., 2013). Yet, there is relatively little information regarding the composition and flux of particulate P (PP) to depth and how this flux changes seasonally and under changing environmental conditions, such as oxygen content and acidity (Benitez-Nelson et al., 2007; Lyons et al., 2011; Sekula-Wood et al., 2012). A variety of compounds are likely to be released in both particulate and dissolved forms into the surrounding water column via cell death and lysis, sloppy feeding, zooplankton repackaging, etc. (Lampert, 1978; Longhurst, 1991; Wilson et al., 2008).

Most research has focused on the relative composition of the total particulate phosphorus (TPP) pool, with little differentiation between inorganic and organic components. Here, we focus on the composition and associations of the sinking particulate inorganic phosphorus (PIP) and particulate organic phosphorus (POP) pools across the oxic/anoxic interface of a seasonally upwelling-dominated continental margin, the Cariaco Basin, Venezuela. Previous research in this region suggests that PIP, on average, comprises just over 50% of the TPP pool and decreases relative to other P components and major elements with increasing depth in the anoxic portion of the water column. In contrast, POP fluxes decrease relative to PIP and major elements in the oxic waters (Benitez-Nelson et al., 2007). Furthermore, the composition of these particles appears to change as well, with phosphonates being preferentially removed relative to P esters (Benitez-Nelson et al., 2004). In order to investigate these changes in more detail, we used a combination of sequential and chemical extraction techniques to examine P speciation and associations in sinking particulate matter.

2.2 Study Site

The Cariaco Basin is located off the northern coast of Venezuela and is the site of the Cariaco Time-Series Program (Figure 2.1). At 160 km long, 70 km wide and 1.4 km deep it is one of the world's largest anoxic marine basins (Thunell et al., 2000; Taylor et al., 2001; Astor et al., 2003; Goñi et al., 2003; Benitez-Nelson et al., 2007). The Basin is connected to the Atlantic Ocean via a 100 m deep sill and two channels: Canal Centinela and Canal de la Tortuge, 146 m and 135 m deep, respectively. These shallow connections reduce water exchange between the Basin and surrounding Caribbean Sea, such that, when coupled with high seasonal production, waters within the Basin are anoxic below ~275 m (Thunell et al., 2000; Astor et al., 2003; Goñi et al., 2003; Benitez-Nelson et al., 2004, 2007).

Primary production occurs primarily within the upper 20-40 m of the water column and the majority of particle generation happens in this oxic zone (Thunell et al., 2000; Scranton et al., 2006; Benitez-Nelson et al., 2007). Primary production is driven by December-April wind-induced coastal upwelling, a regular seasonal occurrence (Goñi et al., 2003; Benitez-Nelson et al., 2007) caused by movement of the Intertropical Convergence Zone (ITCZ) (Thunell et al., 1999, 2000; Müller-Karger et al., 2000, 2001; Taylor et al., 2001; Goñi et al., 2003; Benitez-Nelson et al., 2007). During the summer and fall, primary production decreases due to increasing stratification caused by a reduction in trade wind intensity (Thunell et al., 1999, 2000; Müller-Karger et al., 2000, 2001; Taylor et al., 2001; Goñi et al., 2003; Benitez-Nelson et al., 2007). Non-upwelling periods are marked by higher rainfall, particularly in May, and occurs when the ITCZ is furthest north (Peterson and Haug, 2006; Benitez-Nelson et al., 2007). This period is

therefore also characterized by higher riverine discharge rates in the four rivers that drain directly into the Basin: Tuy, Unare, Neveri and Manzanares (Milliman and Syvitski, 1992; Benitez-Nelson et al., 2007). Subsurface nepheloid layers are likely a major transport mechanism for particles from the mouths of these rivers, where these layers originate, to deep waters of the Basin (Lorenzoni et al., 2009). Coincident with higher precipitation in May are maxima in the annual average terrigenous and particulate organic carbon (POC) fluxes observed in sediment traps located in the center of the eastern Basin (Figure 2.1). This provides additional evidence for the role of nepheloid layers as a likely transport mechanism of terrigenous particles containing inorganic P from coastal to deep waters (Benitez-Nelson et al., 2007; Martinez et al., 2007; Lorenzoni et al., 2009).

The Cariaco Time-Series Program was established in November 1995 as a joint program between five major Venezuelan institutions and three American universities (www.imars.usf.edu/CAR.fp.html). The program's primary purpose is to study the hydrography, biological production and settling flux of particulate matter in the Cariaco Basin. Included in the time-series are monthly measurements of hydrography, inorganic and organic dissolved and particulate carbon and nutrients, primary production, phytoplankton composition (HPLC and microscopy), and zooplankton composition (Astor et al., 2011: Cariaco Time-Series Methods Manual). There are five moored sediment traps located in the center of the Basin that continuously collect sinking particles as well. These monthly observations from the Cariaco Time-Series have led to recent hypotheses that there has been a major shift in the food web from larger diatoms and coccolithophores to smaller species as a result of increasing stratification post 2004.

At the same time, this shift has occurred with a crash in the regional sardine industry allowing for more intense zooplankton grazing, which has been hypothesized to have led to a corresponding increase in particulate organic carbon export (Taylor et al., 2012). Long term and short term shifts in water column biogeochemistry, the near shore location, anoxic deep waters, and the relatively high resolution and comprehensive sampling of the Cariaco Time-Series Program have made this site an ideal place to examine sources, composition and sinks of particulate P in a coastal ecosystem.

2.3 Methods

2.3.1 Sample Collection

Samples were collected using the sediment trap time-series mooring located in the eastern Cariaco Basin at 10°30'N and 64°40'W (Figure 2.1) from November 1995 to October 2010. Sample collection was done from aboard the 75-foot *R/V Hermano Gines* of the Fundación La Salle de Giencias Naturales located on Margarita Island, Venezuela. The mooring contains five traps, Z, A, B, C and D located at 150, 275, 410, 930 and 1200 m depth in the water column, respectively (Thunell et al., 1999, 2000; Taylor et al., 2001; Astor et al., 2003; Goñi et al., 2003). Traps A-D have been in place since 1995 and trap Z was added in 2003. Traps Z and A are located in oxic waters, while traps B-D are located in the anoxic portion of the water column. Each trap is cone-shaped with a 0.5 m^2 opening and baffle top cover (Thunell et al., 2000; Benitez-Nelson et al., 2004, 2007). Each trap holds 13 sample cups that contain a buffered formalin solution to act as a preservative for collected organic matter. A single cup collects for a 1 to 2-week time period. The traps are deployed in 6-month intervals, in May and November (Thunell et al., 1999, 2000; Goñi et al., 2003; Benitez-Nelson et al., 2004, 2007).

Upon collection, the majority of each cup's supernatant was disposed of, along with any apparent "swimmers". The cups were then sealed and refrigerated before processing as no sample analysis is done aboard the ship. It is important to note here that O'Neill et al. (2005) found that, on average, 30% of the total P measured in the traps is within the supernatant of which > 80% is in the form of inorganic P. Using a precision rotary splitter, samples were divided into quarters. The quarter used for analysis was washed three times with deionized water, frozen, dried and ground (Thunell et al., 2000; Goñi et al., 2003; Benitez-Nelson et al., 2007).

2.3.2 Elemental Analyses

Total particulate P (TPP) and particulate inorganic P (PIP) were measured on 1,355 samples using an adaptation of the Aspila ash-hydrolysis method (Aspila et al., 1976). Data from the Benitez-Nelson et al. (2007) is presented in this paper along with more recent data that increases the length of the dataset from 9 to 15 years. Internal spike tests using the modified Aspila method have found P recoveries of a variety of compounds average 82.2 ± 31.4% (Kelly, 2013). Particulate organic P (POP) is estimated by difference (TPP – PIP). As a result of this chemical separation method, each fraction is analytically defined such that the PIP fraction may contain some acid-labile organic P-containing molecules (e.g. simple sugars), whereas the POP fraction may contain inorganic compounds (e.g. pyrophosphates and phosphonates) (Benitez-Nelson, 2000; Benitez-Nelson et al., 2004). To check analytical accuracy and to monitor potential variability during sample analysis, standard reference materials (SRM), NIST #1573a (tomato leaves) and NIST #1646a (estuarine sediment), was analyzed with each run.

These SRM's were chosen for their range in P content relative to the samples and because they span a range of fresh to recalcitrant organic material.

Various sediment trap samples from cruises 4, 6, 8, 9, 11-15, 17-22, 25, 28 and 29 (n = 368) were also analyzed using a modification of the sedimentary extraction (SEDEX) method. SEDEX is a sequential sedimentary extraction procedure for the separation and quantification of the inorganic associations of P within the particulate P pool (Ruttenberg, 1992; Anderson and Delaney, 2000; Faul et al., 2005). This 5 step chemical extraction method divides P into 5 phases: loosely-bound P, oxide-bound P, authigenic P, detrital P, and organic P. Loosely-bound P is the fraction that is easily released into the dissolved phase when washed with $MgCl_2$. The oxide-bound P is released during the second step after it is reduced using citrate dithionite bicarbonate. Authigenic P is extracted with 1 M sodium acetate in step 3 and detrital P with 1 N HCl in step 4. The remaining P is considered organic and is the P that is extracted with 1 N HCl after combustion at 500°C. Soluble reactive P (SRP) was measured on extracts from each phase using UV/Vis spectroscopy (Koroleff, 1983) excluding the oxide-bound step, which was analyzed on a Lachat QuickChem 8000 autoanalyzer. Samples were run in duplicate with standards matrix-matched for each step.

POC, particulate N (PN), biogenic silica (opal) and calcium carbonate ($CaCO_3$) were analyzed in all sediment samples according to the methods described in Astor et al. (2011: Cariaco Time-Series Methods Manual). Lithogenic or terrestrial content was determined indirectly by subtracting the weight of biogenic material (2.5 * organic matter, biogenic silica and carbonate) from the total sample weight (Thunell, 1998).

2.4 Results

2.4.1 Cariaco Time Series (1995-2010)

Data was collected and analyzed from five sediment traps with the upper two traps located in the oxic portion of the water column, 130 m (Trap Z, 11/2003-10/2010) and 225 m (Trap A, 11/1996-10/2010), and the remaining traps located in the anoxic waters below, 400, 800 and 1255 m (Traps B, C and D, respectively, 11/1995-10/2010). Data from cruises and traps 22Z, 22A, 23Z and 23A were excluded from our analyses. During cruise 22 there was a large anoxic event in which the shackles on traps Z and A corroded, most likely contaminating the samples from these traps. Too little material was collected for traps Z and A from cruise 23 to reliably perform analyses. Ranges, averages and standard deviations of major element concentrations and fluxes for each trap depth are presented in table 2.1. All elemental concentrations, i.e. TPP, POC, Opal, etc., varied significantly with a single trap depth, exceeding an order of magnitude in some instances depending on the depth and element of interest. While both PIP and POP concentrations decreased significantly ($p < 0.01$) within the oxic sediment traps, only PIP continued to decrease into the anoxic waters below before remaining relatively constant by a depth of 930 m. Furthermore, PIP concentrations decreased much more rapidly than POP, such that % PIP decreased from 65 to 45% of the TPP pool. At the same time, POC and PN concentrations either increased, decreased or remained relatively stable suggesting preferential accumulation of these compounds throughout the water column.

All elemental fluxes decreased with increasing trap depth (Figure 2.2). While PIP fluxes decreased throughout the oxic and anoxic water column, POP fluxes only decreased significantly below 225 m and had a similar trend to POC and PN. By 1250 m,

PIP fluxes had been reduced by 82% while opal and organic matter fluxed of C, N and P were reduced by 48 to 59%.

In order to better understand temporal differences in P composition and fluxes we parsed the data into upwelling or non-upwelling periods according to Astor et al.'s (2003) definition, where upwelling is defined as the time period when the 21°C isotherm shallows above 80 m. While POP concentrations remained invariant across both upwelling and non-upwelling periods across all depths, PIP concentrations tended to be significantly greater during more stratified periods, consistent with higher concentrations of carbonate and terrestrial material. In contrast, POC, PN and opal concentrations were significantly greater during upwelling periods. Closer examination of the elemental fluxes showed no clear trends seasonally or with increasing trap depth. Finally, PIP and POP fluxes showed no significant long term trends over the length of the entire data set (Figure 2.2). Long term trends observed in the other elemental components have been discussed in detail elsewhere (Taylor et al., 2012; Thunell et al., submitted).

Elemental fluxes of PN and POC were plotted against TPP, PIP and POP fluxes for each sediment trap. TPP versus PN fluxes were dominated by two distinct data trends. Closer examination suggests that these two trends are almost entirely driven by relatively high PIP fluxes. Given previous research indicating a significant flux of terrestrially-derived PIP into the sediment traps (Benitez-Nelson et al., 2007), the data of the trend with the lower N:P ratio was further categorized into low PIP (n = 64) versus high PIP (n = 61) fluxes using an arbitrary cutoff. With the high PIP fluxes removed, TPP versus PN (and PC) ratios were indistinguishable from the canonical Redfield ratio of 106:16:1 (Redfield et al., 1963) (Figure 2.3, open diamonds), suggesting that at least a fraction of

the residual PIP pool is biologically derived. It is important to note, however, that with increasing depth in the water column, the number of samples with PIP fluxes exceeding 0.05 mmol PIP m^{-2} d^{-1} decreased significantly. Elemental ratios of PN: POP fluxes were not significantly different from Redfield in the shallowest (130 m) trap, but increased with increasing depth, consistent with preferential remineralization of POP.

In order to better characterize potential sources of PIP and POP to the sediment traps, PIP and POP fluxes were plotted against other trap constituents, carbonate, opal and terrigenous material. While POP was strongly correlated to all organic and biomineral trap constituents, as has been observed previously, PIP fluxes continued to show two distinct trends demarcated by high and low PIP fluxes. Of particular interest here is that higher PIP fluxes were not necessarily associated with higher terrestrial fluxes, particularly in the Z trap (Figure 2.4). Furthermore, when high PIP fluxes occurred, they dominated the TPP pool, accounting for more than 75% relative to the average % PIP of 45-65% depending on the trap depth. Potential sources of the TPP as a whole was also investigated based upon the data occurring during a period of upwelling or non-upwelling. Terrigenous and CaCO3 fluxes were plotted against TPP fluxes during both periods (Figure 2.5). We found that the distinct splitting pattern in the data only occurs during non-upwelling (Figures 5c and 5d). During periods of upwelling, both terrigenous (Figure 5a, $R^2 = 0.68$) and $CaCO_3$ (Figure 5b, $R^2 = 0.64$) fluxes show a moderately strong linear relationship with TPP.

2.4.2 SEDEX: Breaking down the PIP

To understand the sources and composition of the PIP pool, we conducted a sequential extraction on various samples throughout the time series (1995-2010) from

cruises 4, 6, 8, 9, 11-15, 17-22, 25, 28 and 29. This includes all the SEDEX data available for the time series; as SEDEX is a much more time intensive procedure, the number of samples it has been conducted on is much smaller than the total number of samples we have. Having said this, however, we feel the SEDEX data we do have represents fairly typical conditions of the Cariaco Basin, including several high PIP flux events.

To verify our SEDEX data, SEDEX TPP values were plotted against Aspila TPP values and very good agreement was found ($R^2 = 0.93$; Figure 2.6); this provided the assurance that the SEDEX data was reliable. The PIP SEDEX data was split based upon each sample's PIP flux. Low PIP flux samples were designated as those with fluxes < 0.05 mmol PIP m^{-2} d^{-1} and high PIP flux samples as those with fluxes ≥ 0.05 mmol PIP m^{-2} d^{-1}. The total µmol P/g of each fraction was stacked within each low and high PIP flux group per sediment trap (Z-C; Figure 2.7). Error bars represent ± 1 standard deviation per fraction. By comparing the low PIP flux samples to one another and the high PIP flux samples to one another it is apparent that the high PIP flux samples compositionally vary much more than the low PIP flux samples; variability in average fraction concentrations vary much less in low PIP flux samples than in high PIP flux samples. A two-tailed t-test was used to determine that average concentrations of the fractions between low and high PIP fluxes are significantly different ($p < 0.05$) in each trap. The only occurrences of significant differences ($p < 0.05$) in fraction concentrations within low PIP flux samples are oxide P and detrital P between traps Z and A. Significant differences are seen in all fraction concentrations except detrital P between traps Z and A among high PIP flux samples. Additionally, oxide P concentrations are significantly different between traps Z and B, although it is close to the cut-off ($p = 0.04$).

To gain further perspective of the high and low PIP compositions across the traps, relative percents of the fractions were plotted (Figure 2.8). The relative percent of labile P increases from trap Z to A then decreases from A to C in both the low and high PIP flux samples, though the relative percentage of labile P is greater in the high PIP flux samples. The opposite trend is true for the relative percent of oxide bound P, decreasing from Z to A then increasing from A to C. Labile and oxide bound P clearly dominate both low and high PIP flux samples at all trap depths accounting for > 90% of the IP.

2.5 Discussion

2.5.1 Cariaco Time Series (1995-2010)

Contrary to earlier studies stating that organic P dominates the sinking TPP pool (Benitez-Nelson, 2000), it is shown here that it is, in fact, PIP that contributes the most to the sinking TPP pool. This is in agreement with more recent studies (Paytan et al., 2003; Benitez-Nelson et al., 2007; Lyons et al., 2003) that have seen similar results. PIP's dominance is also evident in figure 2, which illustrates the variability in the PIP and POP fluxes over the time series and with depth. In general, the flux of P decreases due to a combination of particulate remineralization and movement into anoxic waters that reduce oxide associated P.

A pronounced split trend is seen when PN fluxes are plotted against TPP fluxes (Figure 2.3). We believe this second trend in the data (yielding P:N ratios < ~6) is due to a high amount of PIP present. Evidence for attributing the second trendline to PIP is derived from the fact that dates of the data points in the second trendline in both the PIP and TPP plots correspond to one another (open circles, Figure 2.3). Particularly high PIP fluxes are represented by circles and are due to high TPP or PIP concentrations, not

necessarily high mass fluxes. The decrease in the data splitting as you move from shallow, oxic waters (trap Z) to deep, anoxic waters (trap D) indicates a decrease in PIP, potentially due to it being preferentially taken up and remineralized in anoxic waters. This splitting of the data is gone by 1255 m (trap D). The linear trend seen between PN and POP (Figure 2.3) and the closeness of its ratio to that of Redfield confirms the biological (and organic) origin of the POP.

To determine a potential source for this "extra" PIP and subsequent data trends, we compared TPP and PIP fluxes to the terrigenous flux. We found that, once again, there is a split in the data, suggesting that the large amount of PIP contributing to the second trendline is of lithogenic origin (Figure 2.4), however, high terrigenous fluxes do not correlate with high PIP fluxes as we might expect. The split in the data is most pronounced near the surface where the terrigenous material enters the water column (Figures 2.4a and b). Even between traps Z and A the split is noticeably more prevalent in trap Z than in A. We believe this is due to the remobilization of relict sediments on the Unare shelf that are carried out to the trap mooring and collected in trap Z, yielding some especially high PIP values. The reason the split in the data is not as pronounced in trap A is due to the depth at which it sits and the depth of the shelf. The Unare shelf is approximately 100 - 200 m deep, a depth range in which trap Z falls (130 m), however, is too shallow to contribute as much PIP to the deeper traps. Some of this high PIP does reach the deeper traps through a mechanism initially proposed by Lorenzoni et al. (2009). Upon observing intermediate nepheloid layers occurring at the Unare Platform shelf break, they proposed these nepheloid layers as a mechanism for transporting particulate material from the continental shelf to the deep waters of the basin. We believe it is

through this mechanism that some of remobilized lithogenic material reaches the deeper traps and produces the splitting trend we are seeing in these traps. However, this split in the data decreases with increasing depth and disappears upon reaching trap D (Figures 2.4b, c and d). This is likely due to the high PIP being preferentially taken up and removed as it sinks throughout the water column. The appearance of the split in the data only during periods of non-upwelling is expected because during these periods rainfall is higher and biological activity is low, resulting in this high amount of "extra" PIP we are seeing (Figure 2.5).

2.5.2 SEDEX: Breaking down the PIP

The large concentration of PIP in the Z trap of high PIP flux samples is likely attributed to the remobilization of lithogenic material off the Unare Platform at 150-200 m depth. A possible mechanism for the progression of this PIP from the Z trap to deeper traps is intermediate nepheloid layers (near the shelf break, ~100 m) that have been observed in the Cariaco Basin (Lorenzoni et al., 2009). Unlike the PIP in the low PIP flux samples, we know this PIP is not biological in origin due to its ratio with organic C being much lower than the canonical Redfield ratio of 16:1. As there are no correlations between rainfall or earthquakes and the high PIP fluxes, these events are also eliminated as potential sources. The especially high concentration of PIP in the Z trap is most likely due to the remobilization of lithogenic sediments off the Unare Platform at The decrease in concentrations between traps Z and A among the high PIP flux samples is significant ($p < 0.05$) for all the fractions except detrital P (Figure 2.7), perhaps attributable to the uptake of the P by biological activity. PIP concentration, especially labile and oxide bound P, increase from trap A to C; however, according to the t-test, fraction

concentrations between traps A and B and B and C are not significantly different except for oxide bound P concentrations between traps A and B ($p = 0.04$).

Relative percent distributions of the inorganic fractions among the low PIP flux samples and among the high PIP flux samples exhibit a similar trend of labile P increasing from trap Z to A then subsequently decreasing from A to C (Figure 2.8). Conversely, the relative percent of oxide bound P decreases from trap Z to A followed by its increasing from A to C. The increase in relative percent labile P could be explained by zooplankton repackaging and its following decrease by preferential uptake through biological activity. An increase in relative percent oxide bound P from trap A to C is not what we would expect but this increase is not significant as shown by the t-test performed on the average fraction concentrations.

2.6 Conclusions

The PIP fraction in sediment trap samples is perhaps more dynamic than previously thought and should be receiving as much, if not more, attention as the POP fraction. Across the Cariaco time series (1995-2010) we see a distinct splitting trend in the TPP data that can be attributed to 'extra' high PIP. This trend is strongest at the shallowest trap (~130 m) and weakens with increasing depth until its disappearance at the deepest trap (~1250 m). We believe this high PIP is coming from the remobilization of relict sediments (lithogenic in origin) off the Unare platform. Nepheloid layers at the shelf break are the likely mechanism for transporting this high PIP to the deeper traps, although the amount of this PIP present diminishes with depth as it is being preferentially taken up and removed as it sinks. This is evidenced in the PN flux versus TPP flux plots of the traps; the pronounced split in the data seen in trap Z is obviously already

weakening by trap A and subsequently, traps B and C. Associations between TPP fluxes and terrigenous and $CaCO_3$ fluxes suggest terrestrial and carbonate materials are also potential sources of this high PIP. The fact that the splitting trend (and 'extra' high PIP) is only seen during periods of non-upwelling is understandable as these periods are characterized by low biological activity and higher rainfall, both factors leading to less biological sourced material and more inorganic sourced material (e.g. terrestrial material input from increased land run-off due to higher rainfall). Using SEDEX data we found that the labile P and oxide bound P fractions contribute the most to the PIP pool, especially the high PIP ($\geq$ 0.05 mmol PIP m^{-2} d^{-1}) that produces the split in the data. When comparing fraction percentages between low and high PIP fluxes similar trends are observed in the labile and oxide bound P fractions though on a greater scale in the high PIP samples. We've shown there is a lot happening within in the PIP fraction of the TPP pool and thus there needs to be further concentration and investigation into this fraction. Focus needs to shift from only the POP pool to both the PIP and POP pools with equal scrutiny applied to both.

Table 2.1 Measurements of total mass, mineral and elemental concentrations and fluxes in Cariaco Basin sediment trap samples from all trap depths: 130 (Z trap), 225 (A trap), 400 (B trap), 800 (C trap) and 1255 m (D trap).

	Concentration (µmol g^{-1})		Flux[a] (µmol m^{-2} d^{-1})		Concentration (µmol g-1)			Flux[a] (µmol m-2 d-1)		
					Upwelling[b]	Non-upwelling[b]		Upwelling[b]	Non-upwelling[b]	
	Mean ± S.D.	Min − Max	Mean ± S.D.	Min-Max	Mean ± S.D.	Mean ± S.D.	p-value[c]	Mean ± S.D.	Mean ± S.D.	p-value[c]
Z Trap										
TPP	105 ± 118	34 − 890	61 ± 75	8.1 − 695	69 ± 33	120 ± 134	**0.03**	42 ± 21	70 ± 86	0.07
PIP	72 ± 114	13 − 826	41 ± 71	4.5 − 645	36 ± 23	87 ± 131	**0.03**	21 ± 12	49 ± 82	0.06
POP	34 ± 20	3.2 − 120	20 ± 14	1.0 − 72	33 ± 17	33 ± 25	0.98	21 ± 13	20 ± 16	0.89
SEDEX										
Labile	35 ± 54	3.9 − 251	21 ± 35	1.1 − 196	16 ± 12	44 ± 64	0.11	9.9 ± 6.9	26 ± 41	**<0.01**
Oxide	50 ± 91	2.9 − 477	29 ± 63	1.1 − 372	23 ± 17	62 ± 107	0.20	11.9 ± 9.4	37 ± 75	**<0.01**
Authigenic	6.1 ± 6.7	<0.1 − 31	4.4 ± 9.0	<0.1 − 55	3.9 ± 2.1	7.2 ± 7.8	0.12	2.5 ± 2.3	5.3 ± 10.7	0.34
Detrital	0.89 ± 0.48	0.2 − 2.7	0.66 ± 1.09	<0.1 − 7.1	0.79 ± 0.31	0.94 ± 0.54	0.33	0.50 ± 0.36	0.73 ± 1.32	0.52
Organic	22.6 ± 7.8	13 − 50	14 ± 12	2.7 − 66	22.4 ± 5.7	22.7 ± 8.7	0.93	14.5 ± 9.7	14 ± 13	0.87
POC	6784 ± 3027	3049 − 19458	4172 ± 2799	509 − 16076	6300 ± 1386	7176 ± 3631	0.19	4129 ± 2385	4476 ± 3154	0.57
PN	956 ± 505	404 − 3331	583 ± 408	64 − 2210	876 ± 224	1025 ± 609	0.18	572 ± 328	633 ± 476	0.50
Terrigenous	49 ± 13[d]	5.8 − 76[d]	0.36 ± 0.31[e]	<0.1 − 2.2[e]	47.5 ± 8.4[d]	50 ± 14[d]	0.44	0.34 ± 0.23[e]	0.37 ± 0.34[e]	0.55
Opal	8.4 ± 4.0[d]	<0.1 − 28[d]	0.06 ± 0.05[e]	<0.1 − 0.3[e]	8.5 ± 2.2[d]	8.5 ± 4.5[d]	0.97	0.06 ± 0.03[e]	0.06 ± 0.06[e]	0.68
$CaCO_3$	22.8 ± 7.7[d]	10 − 68[d]	0.15 ± 0.12[e]	<0.1 − 0.6[e]	25.1 ± 6.8[d]	20.9 ± 5.3[d]	**<0.01**	0.18 ± 0.14[e]	0.14 ± 0.11[e]	0.13
Total Mass	---	---	0.69 ± 0.52[e]	<0.1 − 3.5[e]	---	---	---	0.69 ± 0.44[e]	0.71 ± 0.55[e]	0.90
A Trap										
TPP	78 ± 71	27 − 1023	58 ± 44	4.6 − 336	64 ± 22	82 ± 81	0.08	42 ± 31	64 ± 46	**<0.01**
PIP	48 ± 55	1.3 − 730	35 ± 31	0.6 − 293	34 ± 21	53 ± 62	**0.02**	23 ± 21	39 ± 34	**<0.01**
POP	30 ± 22	5.5 − 293	23 ± 20	1.4 − 218	30 ± 11	30 ± 25	0.93	20 ± 14	25 ± 22	0.10
SEDEX										
Labile	27 ± 25	3.9 − 114	26 ± 35	0.9 − 198	18 ± 16	31 ± 28	**0.04**	12 ± 14	33 ± 40	**0.01**
Oxide	13.8 ± 8.4	1.3 − 50	14 ± 17	0.8 − 109	10.1 ± 4.9	15.4 ± 9.1	**0.01**	6.4 ± 4.6	17 ± 19	**0.01**
Authigenic	3.7 ± 2.4	0.2 − 15	3.8 ± 4.9	<0.1 − 35	3.6 ± 2.7	3.8 ± 2.3	0.66	2.3 ± 2.1	4.4 ± 5.6	0.07
Detrital	0.75 ± 0.34	0.3 − 2.1	0.73 ± 0.80	<0.1 − 5.5	0.67 ± 0.30	0.78 ± 0.35	0.19	0.42 ± 0.26	0.87 ± 0.91	**0.02**
Organic	21.1 ± 5.4	13 − 41	18 ± 12	3.2 − 71	23.3 ± 5.0	20.0 ± 5.0	**0.01**	14.6 ± 8.3	20 ± 13	0.08
POC	7471 ± 2609	2714 − 18383	5644 ± 3780	246 − 20192	8654 ± 2469	6921 ± 2361	**<0.01**	5589 ± 3761	5812 ± 3732	0.68
PN	950 ± 353	312 − 2650	709 ± 474	34 − 2552	1089 ± 303	877 ± 323	**<0.01**	700 ± 468	730 ± 469	0.66

Terrigenous	52 ± 12[d]	20 – 81[d]	0.47 ± 0.52[e]	<0.1 – 4.5[e]	47 ± 11[d]	54 ± 12[d]	**<0.01**	0.35 ± 0.31[e]	0.53 ± 0.57[e]	**0.02**
Opal	11.2 ± 6.0[d]	<0.1 – 31[d]	0.09 ± 0.08[e]	<0.1 – 0.5[e]	14.1 ± 6.5[d]	10.2 ± 5.6[d]	**<0.01**	0.09 ± 0.07[e]	0.09 ± 0.08[e]	0.99
$CaCO_3$	14.3 ± 4.2[d]	4.0 – 30[d]	0.12 ± 0.09[e]	<0.1 – 0.6[e]	12.7 ± 4.5[d]	14.8 ± 4.0[d]	**<0.01**	0.09 ± 0.07[e]	0.13 ± 0.10[e]	**<0.01**
Total Mass	---	---	0.85 ± 0.74[e]	<0.1 – 5.6[e]	---	---	---	0.69 ± 0.52[e]	0.93 ± 0.79[e]	**0.03**
B Trap										
TPP	63 ± 42	28 – 324	38 ± 27	1.5 – 192	52 ± 21	67 ± 48	**<0.01**	40 ± 25	37 ± 28	0.35
PIP	36 ± 37	0.1 – 253	20 ± 18	<0.1 – 163	23 ± 17	41 ± 42	**<0.01**	17 ± 13	21 ± 20	0.12
POP	27 ± 15	1.4 – 143	18 ± 15	0.1 – 81	29 ± 10	27 ± 17	0.14	23 ± 15	16 ± 14	**<0.01**
SEDEX										
Labile	25 ± 36	2.2 – 215	15 ± 22	0.4 – 138	8.0 ± 6.0	34 ± 42	**<0.01**	7.4 ± 8.5	20 ± 26	**0.01**
Oxide	17 ± 18	1.8 – 135	13 ± 15	0.8 – 78	16 ± 14	18 ± 20	0.53	14 ± 17	12 ± 14	0.65
Authigenic	3.6 ± 2.4	0.6 – 20	2.8 ± 3.2	0.1 – 22	3.2 ± 1.4	3.8 ± 2.7	0.22	2.8 ± 2.3	2.8 ± 3.6	0.96
Detrital	0.75 ± 0.39	0.3 – 3.3	0.57 ± 0.53	<0.1 – 3.1	0.71 ± 0.30	0.78 ± 0.43	0.38	0.59 ± 0.37	0.57 ± 0.61	0.92
Organic	19.0 ± 5.3	8.8 – 38	14 ± 11	1.7 – 46	21.5 ± 6.8	17.4 ± 3.5	**<0.01**	18 ± 12	12.3 ± 9.6	**0.01**
POC	7207 ± 2420	2852 – 17283	4575 ± 3456	218 – 20711	8237 ± 2461	6681 ± 2203	**<0.01**	6457 ± 4072	4010 ± 2876	**<0.01**
PN	873 ± 292	327 – 1889	554 ± 415	26 – 2436	1003 ± 305	807 ± 262	**<0.01**	778 ± 475	487 ± 353	**<0.01**
Terrigenous	52 ± 11[d]	23 – 81[d]	0.37 ± 0.37[e]	<0.1 – 3.0[e]	48 ± 11[d]	54 ± 11[d]	**<0.01**	0.41 ± 0.31[e]	0.38 ± 0.39[e]	0.51
Opal	12.4 ± 6.1[d]	<0.1 – 33[d]	0.09 ± 0.09[e]	<0.1 – 0.5[e]	15.6 ± 5.8[d]	11.2 ± 5.9[d]	**<0.01**	0.13 ± 0.10[e]	0.07 ± 0.07[e]	**<0.01**
$CaCO_3$	13.7 ± 4.7[d]	0.7 – 30[d]	0.09 ± 0.08[e]	<0.1 – 0.6[e]	12.2 ± 4.4[d]	14.7 ± 4.5[d]	**<0.01**	0.11 ± 0.09[e]	0.09 ± 0.08[e]	0.17
Total Mass	---	---	0.68 ± 0.58[e]	<0.1 – 3.8[e]	---	---	---	0.84 ± 0.58[e]	0.67 ± 0.57[e]	**0.02**
C Trap										
TPP	64 ± 49	4.9 – 373	26 ± 29	1.8 – 281	56 ± 37	67 ± 52	0.08	30 ± 39	25 ± 23	0.23
PIP	36 ± 44	0.9 – 353	14 ± 16	0.1 – 117	28 ± 37	40 ± 46	**0.04**	13 ± 16	14 ± 15	0.72
POP	28 ± 19	0.7 – 156	13 ± 18	<0.1 – 206	28 ± 13	27 ± 21	0.70	17 ± 27	11 ± 12	**0.02**
SEDEX										
Labile	19 ± 47	2.6 – 390	10 ± 21	0.5 – 161	11 ± 13	25 ± 60	0.16	8.7 ± 17.0	12 ± 24	0.53
Oxide	21 ± 30	3.4 – 234	11 ± 16	1.2 – 107	24 ± 27	19 ± 33	0.46	15 ± 21	9.1 ± 12.1	0.07
Authigenic	3.9 ± 4.3	0.6 – 27	2.6 ± 4.7	0.4 – 34	4.0 ± 5.0	4.0 ± 3.9	0.98	2.6 ± 3.4	2.6 ± 5.4	0.99
Detrital	0.72 ± 0.40	0.2 – 2.5	0.43 ± 0.52	<0.1 – 3.6	0.70 ± 0.47	0.72 ± 0.36	0.83	0.46 ± 0.48	0.42 ± 0.56	0.77
Organic	19.0 ± 6.0	5.6 – 43	12 ± 18	2.2 – 149	22.0 ± 7.1	17.1 ± 4.3	**<0.01**	17 ± 26	9.5 ± 8.0	**0.04**
POC	7765 ± 2828	2424 – 17208	3428 ± 4995	123 – 70397	9469 ± 2769	6871 ± 2370	**<0.01**	5358 ± 8436	2921 ± 2283	**<0.01**
PN	928 ± 371	289 – 2482	412 ± 597	19 – 8413	1153 ± 360	808 ± 297	**<0.01**	646 ± 1005	344 ± 269	**<0.01**
Terrigenous	51 ± 12[d]	22 – 82[d]	0.26 ± 0.38[e]	<0.1 – 3.4[e]	45 ± 10[d]	54 ± 11[d]	**<0.01**	0.28 ± 0.37[e]	0.28 ± 0.39[e]	0.94

Opal	12.5 ± 6.4[d]	<0.1 − 37[d]	0.07 ± 0.11[e]	<0.1 − 1.5[e]	16.5 ± 6.6[d]	11.1 ± 5.7[d]	**<0.01**	0.11 ± 0.18[e]	0.05 ± 0.05[e]	**<0.01**
$CaCO_3$	12.9 ± 5.2[d]	0.1 − 30[d]	0.06 ± 0.10[e]	<0.1 − 1.2[e]	9.7 ± 5.4[d]	14.4 ± 4.6[d]	**<0.01**	0.07 ± 0.15[e]	0.07 ± 0.07[e]	0.77
Total Mass	---	---	0.48 ± 0.66[e]	<0.1 − 7.4[e]	---	---	---	0.62 ± 0.93[e]	0.49 ± 0.54[e]	0.16
D Trap										
TPP	61 ± 57	7.3 − 565	18 ± 16	<0.1 − 127	54 ± 28	64 ± 66	0.23	19 ± 18	19 ± 16	0.75
PIP	33 ± 57	4.4 − 551	8.5 ± 9.8	<0.1 − 80	24 ± 22	37 ± 67	0.11	8.4 ± 11.2	9.1 ± 9.4	0.63
POP	28 ± 13	<0.1 − 88	9.6 ± 9.3	<0.1 − 68	30 ± 14	27 ± 14	0.38	11.0 ± 9.2	9.5 ± 9.5	0.29
SEDEX										
Labile	7.8 ± 5.2	2.1 − 25	4.0 ± 5.0	0.7 − 25	6.2 ± 2.9	9.2 ± 6.3	**0.03**	3.2 ± 4.7	4.3 ± 4.4	0.38
Oxide	10.4 ± 5.7	2.1 − 28	6.4 ± 12.1	0.6 − 83	8.7 ± 6.0	11.2 ± 4.8	0.07	5.2 ± 10.6	5.2 ± 3.0	0.96
Authigenic	3.1 ± 2.0	0.8 − 11.3	2.2 ± 5.4	0.2 − 32	2.8 ± 2.1	3.2 ± 1.9	0.38	2.2 ± 6.0	1.5 ± 1.0	0.51
Detrital	0.76 ± 0.32	0.3 − 2.4	0.46 ± 0.81	<0.1 − 4.9	0.74 ± 0.30	0.77 ± 0.34	0.72	0.45 ± 0.85	0.35 ± 0.20	0.53
Organic	19.9 ± 5.7	8.1 − 39	10.0 ± 8.7	1.9 − 54	22.3 ± 6.2	18.0 ± 4.2	**<0.01**	10.2 ± 8.3	8.7 ± 5.0	0.38
POC	8508 ± 3216	1121 − 18183	2396 ± 2156	30 − 15507	9936 ± 3281	7635 ± 2760	**<0.01**	3465 ± 2417	2570 ± 2037	**<0.01**
PN	1206 ± 948	81 − 8053	340 ± 434	7.1 − 4121	1201 ± 391	1171 ± 1108	0.84	416 ± 276	398 ± 536	0.79
Terrigenous	50 ± 14[d]	3.1 − 100[d]	0.19 ± 0.37[e]	<0.1 − 3.8[e]	43 ± 13[d]	52 ± 12[d]	**<0.01**	0.21 ± 0.43[e]	0.21 ± 0.28[e]	0.95
Opal	12.0 ± 7.5[d]	<0.1 − 50[d]	0.04 ± 0.04[e]	<0.1 − 0.3[e]	16.9 ± 7.0[d]	11.4 ± 7.1[d]	**<0.01**	0.06 ± 0.05[e]	0.04 ± 0.04[e]	**<0.01**
$CaCO_3$	13.1 ± 5.7[d]	<0.1 − 37[d]	0.04 ± 0.05[e]	<0.1 − 0.4[e]	10.8 ± 4.8[d]	13.9 ± 5.1[d]	**<0.01**	0.04 ± 0.03[e]	0.05 ± 0.05[e]	0.13
Total Mass	---	---	0.32 ± 0.47[e]	<0.1 − 4.5[e]	---	---	---	0.41 ± 0.54[e]	0.38 ± 0.41[e]	0.63

[a]Fluxes were calculated as the product of element concentration (µmol g-1) and total mass flux (g m-2 d-1).

[b]Data were divided into upwelling and non-upwelling periods, where upwelling is defined as the time period when the 21°C isotherm shallows above 80 m (Astor et al., 2003).

[c]Significance was tested using a t-test with p-values < 0.05 in bold.

[d]Weight %

[e]Units are g m^{-2} d^{-1}

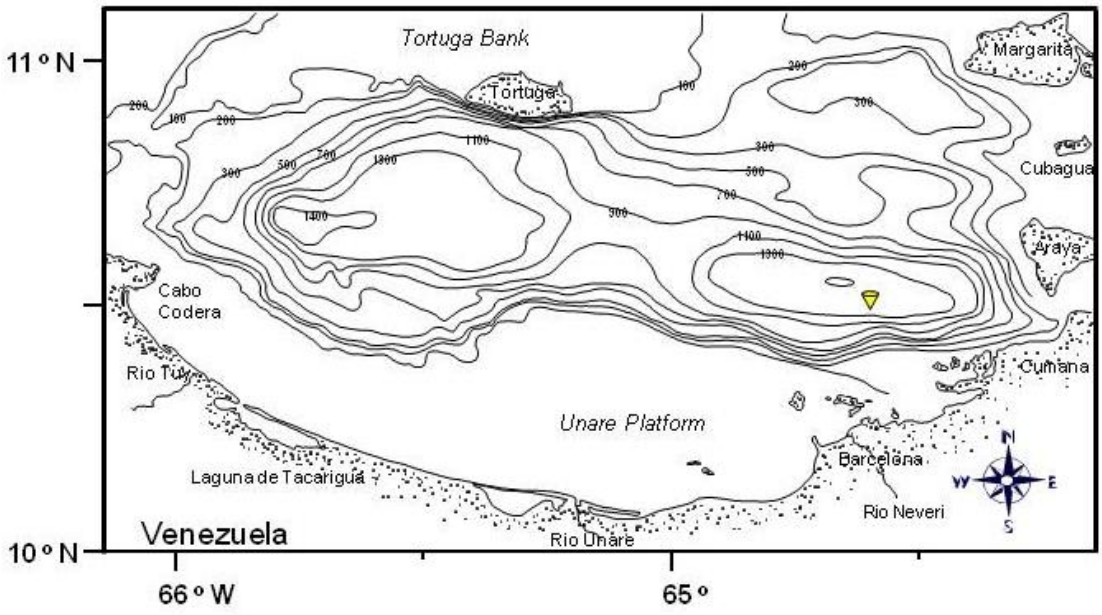

Figure 2.1 Map of the Cariaco Basin off the northern coast of Venezuela denoting the position of the sediment trap mooring (yellow inverted cone) within the study site at 10°30'N and 64°40'W on the eastern side of the Basin (photo credit: Eric Tappa).

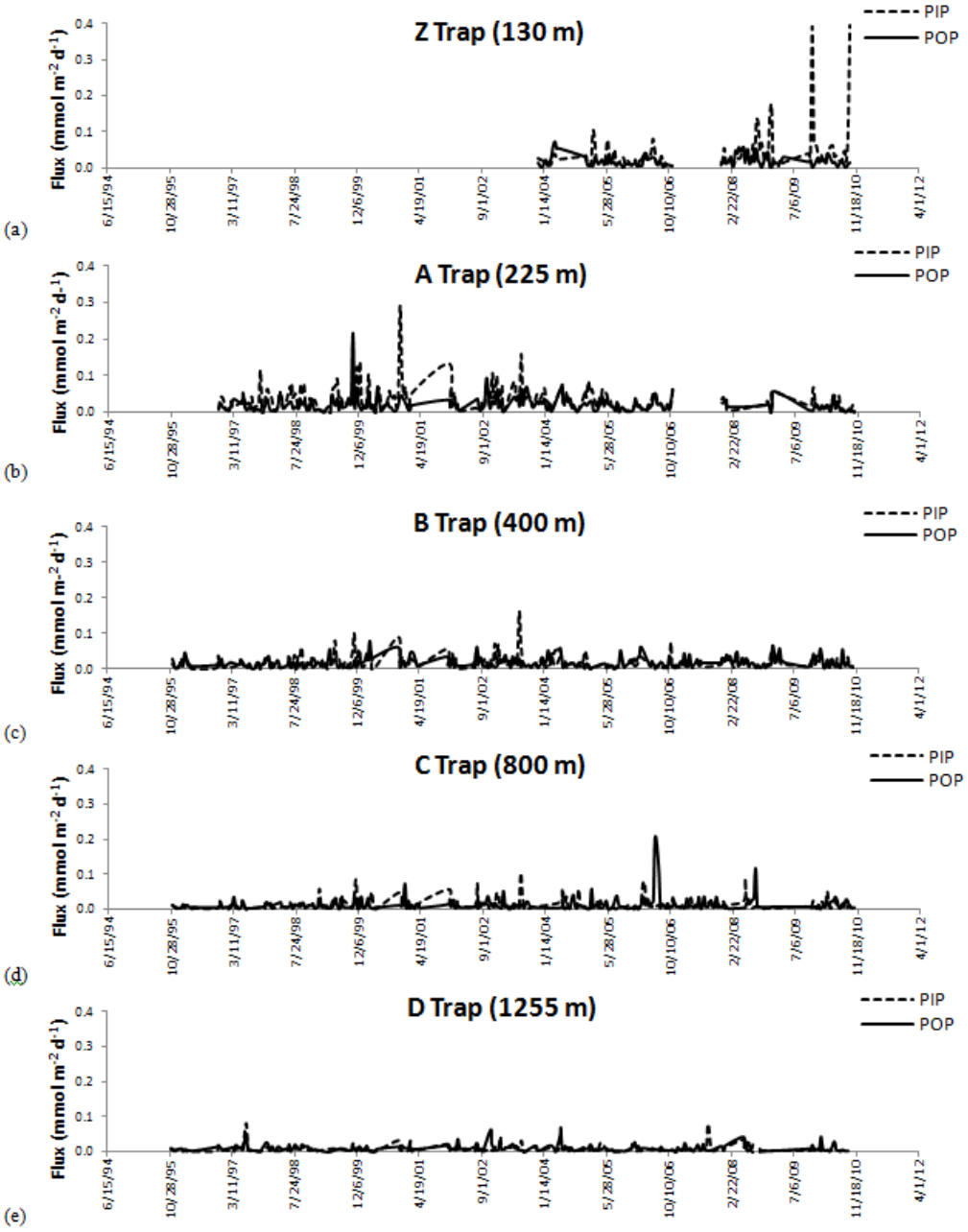

Figure 2.2 PIP (dashed line) and POP (solid line) fluxes (mmol m^{-2} d^{-1}) over The Cariaco time series (1995-2010) for traps Z (a), A (b), B (c), C (d) and D (e). Note that data does not begin for trap Z until the end of 2003 due to the trap not being put into place until November 2003.

(a) Oxic (<250 m)

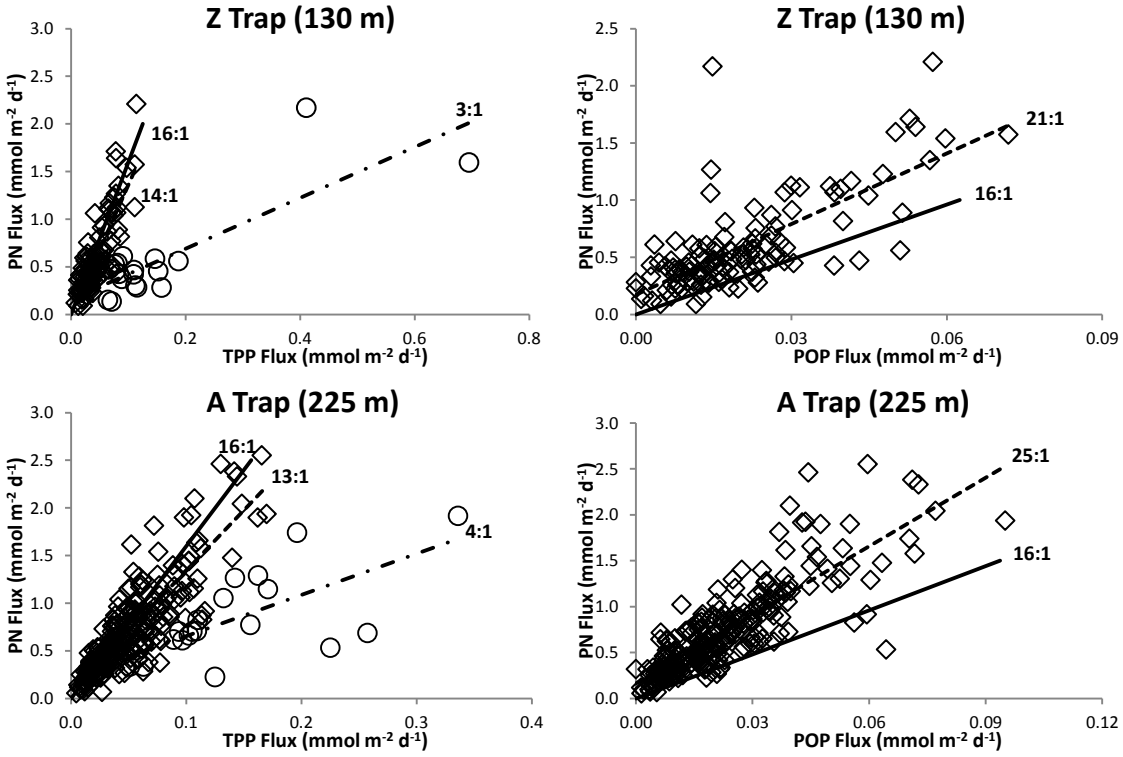

(b) Anoxic (>250 m)

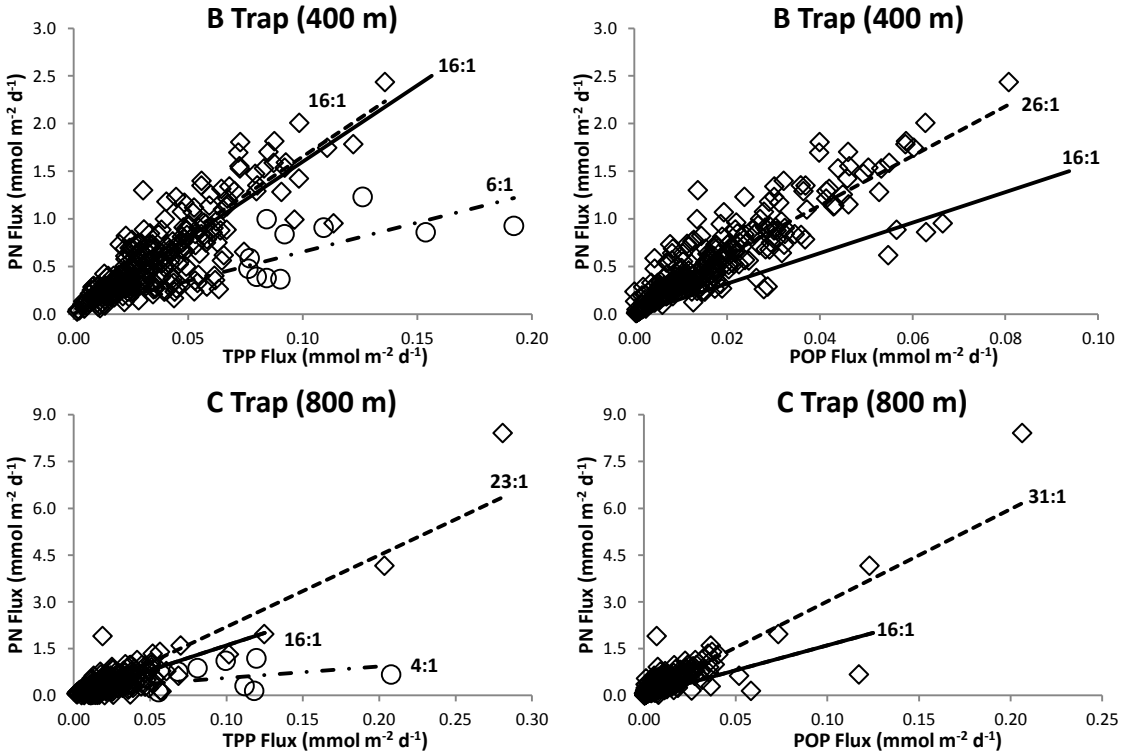

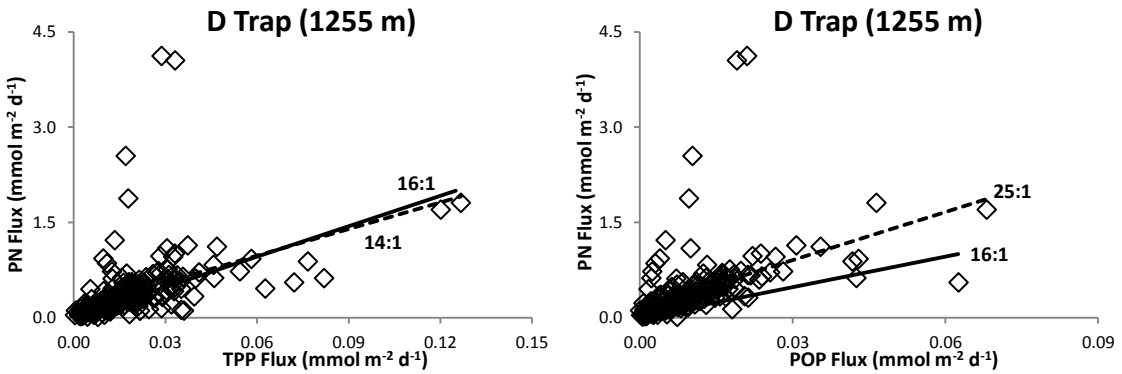

Figure 2.3 PN flux (mmol m^{-2} d^{-1}) versus TPP and POP fluxes (mmol m^{-2} d^{-1}) for the Cariaco time series (1995-2010). Traps Z and A are located in the oxic part of the water column (a) and traps B, C and D are in the deeper, anoxic waters (b). The data points represented as circles in the plots for traps Z – C are dates that are characterized by high PIP fluxes (> 0.05 mmol m^{-2} d^{-1}) and contribute to the second trendline seen in the TPP plots. The solid line represents the Redfield P:N ratio of 16:1; the dashed line is the best fit line that the majority of the data follow and is close to the Redfield ratio line; the dash-dot-dash line is the best fit line for the data producing the second trend seen due to high PIP concentrations and thus lower P:N ratios. The second trend is absent in trap D, reaching only as deep as the C trap.

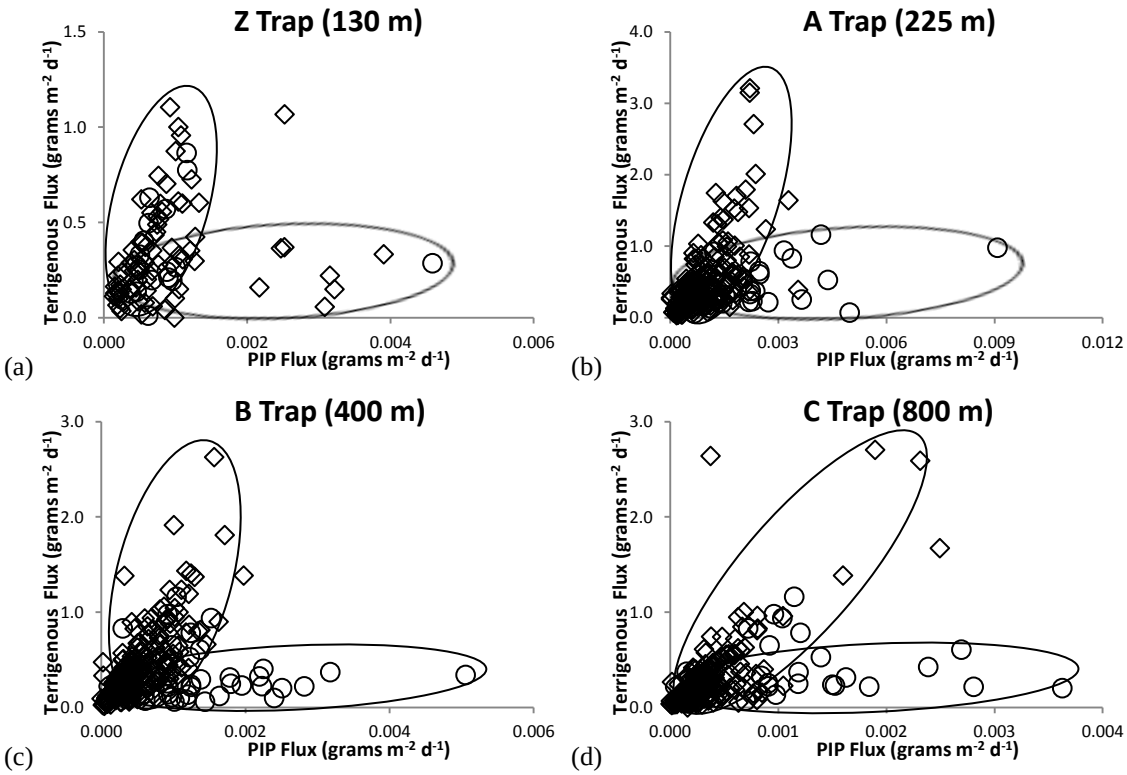

Figure 2.4 Terrigenous flux (grams m^{-2} d^{-1}) versus PIP fluxes (grams m^{-2} d^{-1}) for the Cariaco time series (1995-2010) for traps Z (a), A (b), B (c) and C (d). The ovals are overlain on the data to emphasize the occurrence of two trends. Diamonds represent the majority of the samples that fall along the Redfield P:N ratio line in Figure 3. Circles represent the samples with high PIP fluxes that create the second trend in the data seen in Figure 3.

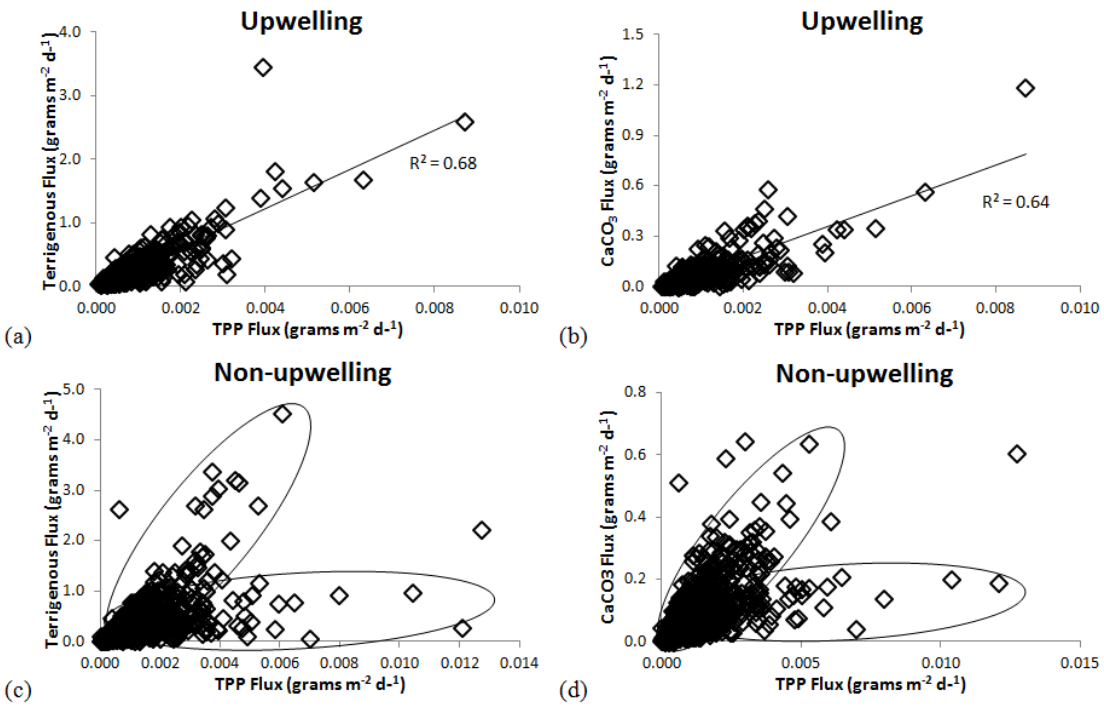

Figure 2.5 Terrigenous and $CaCO_3$ (grams m^{-2} d^{-1}) fluxes versus TPP fluxes (grams m^{-2} d^{-1}) during periods of upwelling (a and b) and non-upwelling (c and d) for the Cariaco time series (1995-2010). Data was split into upwelling and non-upwelling using the definition put forth by Astor et al. (2003).

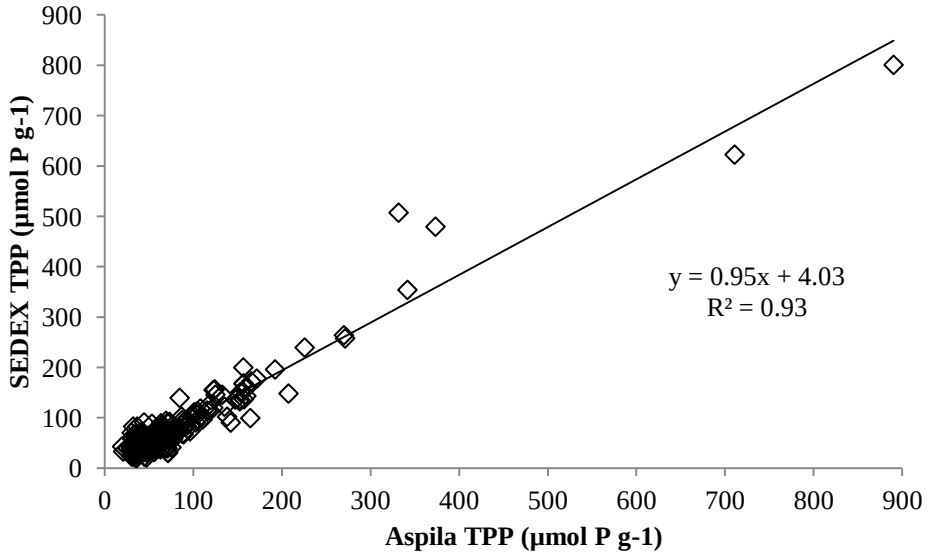

Figure 2.6 SEDEX TPP (µmol P/g) versus Aspila TPP (µmol P/g) of Cariaco sediment trap samples from various cruises (4, 6, 8, 9, 11-15, 17-22, 25, 28 and 29) from 1995-2010 (n = 368).

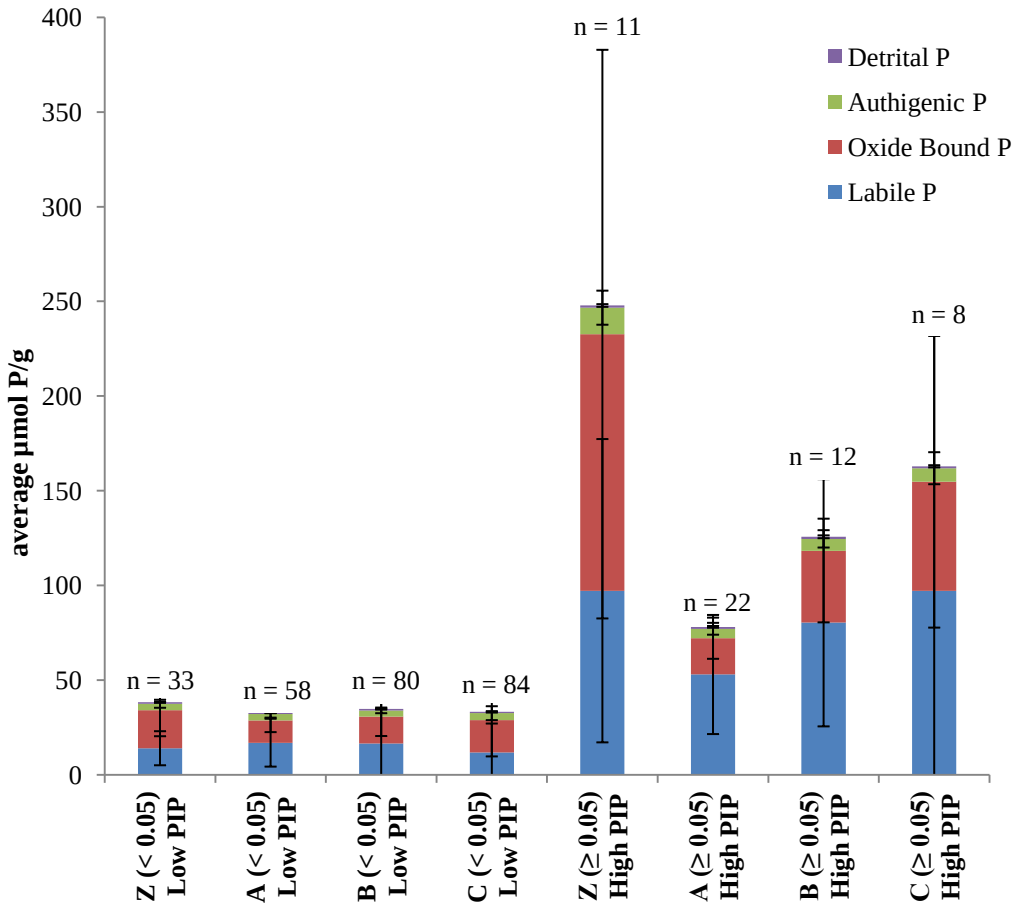

Figure 2.7 SEDEX PIP fractions (detrital P, authigenic P, oxide bound P and labile P) distributions (averages) in low PIP flux (< 0.05 mmol PIP m^{-2} d^{-1}) and high PIP flux (≥ 0.05 mmol PIP m^{-2} d^{-1}) sediment trap samples in traps Z-C. Error bars (± 1 standard deviation) are included for each fraction.

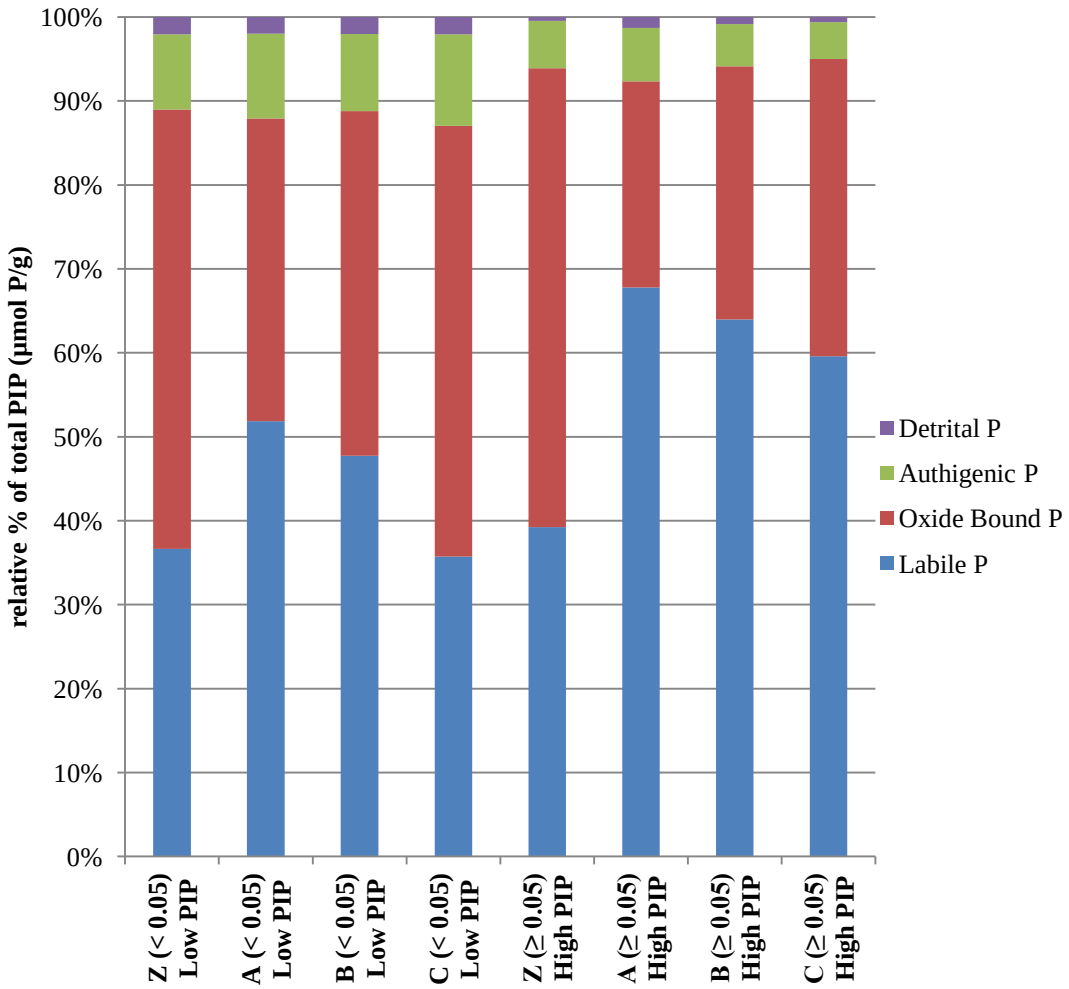

Figure 2.8 Relative percent distributions of the SEDEX PIP fractions (detrital P, authigenic P, oxide bound P and labile P) over each trap (Z-C) for low (< 0.05 mmol PIP m^{-2} d^{-1}) and high (≥ 0.05 mmol PIP m^{-2} d^{-1}) PIP flux sediment trap samples.

CHAPTER 3: ^{31}P-NMR AND MIYATA & HATTORI

3.1 Introduction

Phosphorus (P) is an essential macronutrient used by all marine organisms for growth and energy transport. Yet we still know relatively little about the composition of particulate P (PP) in marine systems. The majority of these studies tend to focus on bulk P measurements and assume that all PP is comprised of particulate organic P (POP). Yet more recent evidence has found that PP is a complex mixture of both inorganic (PIP) and organic components. Although much rarer, studies that do investigate P composition use a variety of chemical extractions, mass spectrometry, ultraviolet/visible (UV/VIS) spectroscopy, high performance liquid chromatography (HPLC), ^{31}P nuclear magnetic resonance (NMR) spectroscopy and X-ray absorption near edge structure (XANES) spectroscopy (Beauchemin et al., 2003; Haberer and Brandes, 2003; Diaz et al., 2008). For example, Diaz and Ingall (2010) developed a polyphosphate method that employs the interaction between 4',6-diamidino-2-phenylindole (DAPI), a fluorochrome, and the polyphosphate.

A method that has been in existence for almost 30 years but is rarely as utilized due to the extensive and time consuming nature of the technique, examines organic phosphorus fractionation, the Miyata & Hattori (1986) method. This technique was modified by DuBois (2008) and some of the fractions combined and redefined based on known compound analysis. Here, the method has been further optimized by examining a series of P standard compounds and examining their actual partitioning with anticipated

results. Sediment traps samples collected from the Cariaco Basin sediment trap time-series program were then analyzed.

In addition, two extraction methods (0.25 M NaOH/0.05 M EDTA and 0.1 M NaAc (pH 5)/Na dithionite) were tested in conjunction with liquid ^{31}P-NMR spectroscopy. P compounds were spiked directly into 0.25 M NaOH/0.05 M EDTA and analyzed using liquid ^{31}P-NMR to verify published chemical shifts. 0.1 M NaAc (pH 5)/Na dithionite also produces accepted chemical shifts of various P compounds yet extracts P better from sediments and thus was chosen to test the extraction efficiency of specific P compounds using liquid ^{31}P-NMR spectroscopy. These compounds were spiked directly into sediments and extracted. Spike samples subjected to the Miyata & Hattori method were then analyzed using ^{31}P-NMR to verify the presence and intact nature of the P compounds tested. Although these results are relatively minimal, they suggest that the combination of these techniques offers promise in determining PP composition.

3.1.1 Miyata & Hattori

A fractionation method of phosphorus components in phytoplankton was developed by Miyata and Hattori (1986). The method uses a combination of acid and charcoal treatments and an organic solvent extraction. Originally Miyata and Hattori applied this method to natural phytoplankton populations and divided cellular phosphorus into orthophosphate, nucleotide P, sugar phosphates, acid-soluble polyphosphates, lipid P, nucleic acid P, acid-insoluble polyphosphates and residual P. They successfully recovered 94±5% of the P and found nucleic acid P and orthophosphate to be the most abundant fractions.

The application of this method to sediment trap samples was investigated by Suzanne DuBois (2008). P standards were spiked into Santa Barbara Basin sediment trap samples and extracted with near 100% recovery, however, they did not necessarily extract into the expected fractions. Given the misidentification, DuBois reclassified and combined the acid-soluble P, nucleotide P, sugar P and orthophosphate fractions collectively under the fraction name of acid soluble P.

3.1.2 What is Nuclear Magnetic Resonance (NMR) Spectroscopy?

NMR spectroscopy uses the magnetic properties of certain atomic nuclei. This technique is applicable to liquid and solid samples and can differentiate the compound groups found within organic and inorganic chemical species (Sannigrahi, 2005). More specifically, FT (Fourier Transform) NMR is commonly used. FT refers to the method used for obtaining readable spectra from the raw data; in more technical terms, the time-domain signal is transformed to a frequency-domain spectrum. The final spectrum displays intensity versus frequency (Holmes, 2004; Sannigrahi, 2005).

In NMR spectra, the frequency at which a nucleus resonates is called its chemical shift (represented by δ). A nucleus' chemical shift depends on its orientation with respect to the external magnetic field (Holmes, 2004). In other words, a chemical shift is equal to the difference between the external applied magnetic field and what the nucleus actually feels (Sannigrahi, 2005). Compounds and/or compound classes have distinctive chemical shifts allowing for the identification of specific components within a sample. Mathematically, chemical shift is defined by the equation,

$$\delta = [(\nu - \nu_0)/\nu_0] \times 10^6$$

where ν is the resonance frequency of the nucleus being studied and ν_0 is the resonance frequency of a reference standard (Sannigrahi, 2005). Due to their very small values, chemical shifts are multiplied by 10^6 to make them more manageable and are thus reported in ppm (Holmes, 2004).

According to Holmes (2004) the following are the most important parameters in NMR:

1. Spectrometer frequency [sfrq]: This frequency pulse is what excites the nuclei in the sample; the nuclei re-emit this pulse throughout the acquisition time (see parameter 3). A NMR signal is provided by the re-emitted pulse in the form of a decaying sine wave, also known as free induction decay (FID). The frequency characterizing this pulse is known as the spectrometer frequency, a parameter dependent on the nucleus of interest and the magnetic field strength of the NMR.
2. Pulse width [pw]: A pulse width is the time interval (measured in microseconds) for which the energy pulse is applied to the sample. Standard protocol is to use a 45° pulse.
3. Acquisition time [at]: This is the time it takes for the nuclear spins to return to their stable states (equilibrium) after excitation and is represented by a decaying sine wave (FID).
4. Number of points [np]: The analog FID collected is translated into individual points along the curve. When the number of points used for the FID curve is increased, resolution improves.

5. Spectral window [sw]: This is the length of the spectrum chosen to display, most commonly in ppm though Hertz (Hz) can also be used. An advantage to using ppm is the window's independence from the operating frequency. The number of Hz per ppm changes with different operating frequencies; therefore the spectral width in Hz is dependent on the instrument being used.
6. First (relaxation) delay [d1]: The relaxation delay occurs after the frequency pulse, which provides the time needed for the nuclear spins to come back to a steady state.

There are two techniques important to NMR that an investigator needs to become proficient at: phasing and shimming. Upon initial analysis, spectra are out of phase or below the baseline. Phasing is the technique used to correct these deviations and ultimately achieve a Laurentian shape for all peak spectra. To achieve this, two phasing parameters need to be adjusted: the 0-order (frequency independent) and 1-order (frequency dependent) phases. Shimming is by far the more difficult of the two techniques; improvements in shimming ability takes time and is mastered with practice and repetitiveness. The purpose of shimming is to produce a magnetic field across the sample that is as homogenous as possible. Homogeneity is gauged by the lock signal; an increase in lock signal means greater homogeneity of the magnetic field. This is a skill that is primarily required at the beginning of the experiment, but is likely to be needed throughout the entire sample run (Holmes, 2004).

3.1.3 ^{31}P-NMR

Phosphorus only has one naturally occurring isotope: ^{31}P. Due to this isotope's 100% natural abundance and its positive ½ nuclear spin, P is easily detected by ^{31}P-NMR

spectroscopy (Paytan et al., 2003). Chemical shifts of P compounds are compared to an external standard, usually phosphoric acid for liquid phases and potassium phosphate salt (K_2PO_4) for solids. The widespread resonance frequency and magnetic field strength used for ^{31}P-NMR is 202.4 MHz and 11.75 T, respectively. Probes with diameters of 5 and 10 mm are the most common, typically holding sample sizes of tenths of 1 to several mL. As it is common for phosphorus concentrations to be quite low in natural samples, the use of a Cryoprobe, instead of a traditional probe, can be used on the instrument to increase sensitivity, which is beneficial for measuring low concentrations. The Cryoprobe does this by cooling the temperature of the sample and thus reducing the background noise, allowing for a stronger signal from the sample (Bruker website). One dimensional (1D) ^{31}P-NMR is most common and sufficient for the majority of analyses. Two dimensional (2D) is possible, but not utilized nearly as much as 1D (Twyman, 2005).

Table 3.1 and figure 3.1 show average chemical shift ranges (ppm) of P compound classes and some P compounds. The chemical shifts of P compounds cover a range of approximately -30 to 30 ppm and are dependent on the matrix of the sample being analyzed.

Solid-state ^{31}P-NMR offers two distinct advantages over solution ^{31}P-NMR: there is little to no sample preparation and the sample remains intact, allowing for further analyses and no assumptions about specific compound extraction efficiencies (Paytan et al., 2003; Sannigrahi et al., 2006). Disadvantages include low resolution spectra with broad peaks that do not allow in identification. Only P compound classes, as opposed to individual P compounds, can be identified with solid-state ^{31}P-NMR (Cade-Menun et al., 2005). The disadvantages that come with using solid-state ^{31}P-NMR can be offset with

solution ^{31}P-NMR. The higher resolution spectra that can be obtained using solution ^{31}P-NMR allow the investigator to determine specific P compounds present in the sample (Cade-Menun and Preston, 1996; Paytan et al., 2003). The drawbacks of solution ^{31}P-NMR are the extensive sample preparation and destruction of the sample; therefore all other analyses must be completed on the sample prior to using solution ^{31}P-NMR (Sannigrahi et al., 2006). Thus, using solid and liquid state ^{31}P-NMR together is ideal.

3.1.4 ^{31}P-NMR in Marine Systems

In marine systems, ^{31}P-NMR is perhaps not as widely used in PP research as it could potentially be. ^{31}P-NMR in marine system studies has only become prevalent in the past 10-15 years, especially liquid state. Contrary to what was previously thought, solid state ^{31}P-NMR results suggest that phosphonates and P esters, not just esters alone, comprise a substantial portion of the TPP pool. Distinctions between ortho- and pyrophosphates and mono-and diesters have been possible due to the sensitivity offered by liquid ^{31}P-NMR, something unattainable from solid state alone. From studies published thus far (see next two sections), it is obvious this instrument can offer great value in studying PP, especially solid and liquid state used together, and in conjunction with other techniques, like chemical extractions.

3.1.4.1 Solid state

DOP composition varies little from 80-85% P esters, 5-10% phosphonates and 8-13% polyphosphates in oligotrophic to eutrophic waters (Young and Ingall, 2010). P esters are the dominant compound class and organic P composition shows little variation with depth in UDOM and UPOM (Sannigrahi et al., 2006).

Phosphate, phosphonates and P esters from sediment traps and cores are present at all water depth and down to 2 cm sediment depth. Despite previous belief, phosphonates comprise a significant portion of the TPP pool at 3-23% (Benitez-Nelson et al., 2004). P esters and phosphonates dominate HMW DOP in surface waters, yet the amount of P esters is three times that of phosphonates (Clark et al., 1998; Kolowith et al., 2001). Both of these P compound classes continue to dominate from surface to deep waters, where they are remineralized at equal rates (Clark et al., 1998, 1999). Phosphonates have been confidently identified in marine POM (Paytan et al., 2003; Benitez-Nelson et al., 2004; Dyhrman et al., 2009). Dyhrman et al. (2009) studied six kinds of cyanobacteria (*T. erythraeum, T. theibauti, T. tenue, Crocosphaera watsonii,* Diatom and Coccolithophore) via solid-state ^{31}P-NMR and only identified the P-C bond unique to phosphonates in cultures of *Trichodesmium erythraeum*. Total phosphonate in these cultures has a positive correlation with TPP. Within these cyanobacteria phosphonates, on average, account for 10% of their cellular PP. These findings suggest that *T. erythraeum* are capable of producing phosphonates (Dyhrman et al., 2009).

Polyphosphates are only found in surface sediments of oxic waters, no deeper than 2 cm, and account for 8% of the total P (Sannigrahi and Ingall, 2005). In the characteristically low P Sargasso Sea, polyphosphates contribute 8-25% of the total P found within *Trichodesmium* (Orchard et al., 2010).

3.1.4.2 Liquid state

The conversion of organic P to inorganic P is substantial, resulting in a significant portion of sinking PP being classified as PIP. P species differ in their relative distributions within POP and plankton material (Paytan et al., 2003). Pyrophosphate can

be recognized from other orthophosphate compounds, a distinction that cannot be made using solid-state ^{31}P-NMR (Cade-Menun et al., 2005).

Liquid ^{31}P-NMR is especially useful for studying and distinguishing the differences between mono- and diesters (Cade-Menun et al., 2005). Oxygenated environments are more conducive to breaking down P diesters to monoesters. This is evidenced by smaller diester peaks and larger monoester peaks in the spectra of samples from these oxygenated environments (Carman et al., 2000).

3.2 Methods

3.2.1 ^{31}P-NMR

Sample preparation for solution ^{31}P-NMR analysis requires chemical extraction procedures. That can take up to 3-4 days. The most commonly used extraction method is 0.25 M NaOH/0.05 M EDTA (Cade-Menun and Preston, 1996). However, other extraction protocols have been used to ensure better extraction efficiencies for specific compounds. For example, sample extraction in 0.1 M NaAc (pH 5)/Na dithionite has been shown to be more adept at extracting phosphonates (He et al., 2009). The first step that requires a significant amount of time is the extraction itself. Samples (suspended in the extractant) are placed on a shaker for 6 to 20 hours or overnight. Following the extraction, filtering is necessary to ensure all particles and solids are removed from the supernatant. The remaining solids are washed with distilled and deionized water (DIW) and these washes are added to the supernatant. Most, if not all, of the sample solution is thoroughly frozen, ~24 hours to ensure the sample is thoroughly frozen. The frozen samples are then freeze-dried which can take anywhere between 24 and 48 hours depending on the volumes of the samples. The last step prior to analysis via solution ^{31}P-

NMR is to dissolve the freeze-dried samples to a volume of ~3 mL, with solutions and volumes used for the final dissolution varying between the chemical extractions used.

3.2.1.1 0.25 M NaOH/0.05 M EDTA

Stock solutions (~200 mM P) were prepared of specific P compounds (sodium phosphate, tripolyphosphate, glucose-6-phosphate, pyrophosphate, glyphosate, adenosine triphosphate (ATP), 2-aminoethylphosphoric acid (AEP), glycerophosphate, pinacolyl methylphosphonate, ethyl methylphosphonate, dimethyl methylphosphonate and sodium polyphosphates (5P, 15P, 60P, 130 P chain lengths)); quantities of these stock solutions were then spiked directly into the 0.25 M NaOH/0.05 M EDTA matrix to yield concentrations ranging from 1 to 10 mM P for each compound. The spikes were then analyzed using liquid ^{31}P-NMR.

3.2.1.2 0.1 M NaAc (pH 5)/Na dithionite

Stock solutions (~200 mM P) were prepared of the specific P compounds (ATP, DNA, RNA, phytic acid, sodium hexametaphosphate and phosphatidylcholine). Initially, 'x' grams of each compound (to yield a final concentration of ~29 mM P) were combined and homogenously mixed with ~0.05 g estuarine sediment. Each sample was then extracted following the protocol using 0.1 M NaAc (pH 5)/Na dithionite (He et al., 2009) and their spectra obtained following analysis using liquid ^{31}P-NMR. For comparison, and to help identify the peaks attributable to the P compound of interest, these compounds were also directly spiked into the extractant and analyzed via ^{31}P-NMR.

3.2.2 Miyata & Hattori

The Miyata & Hattori (1986) method (Figure 3.2) separates POP into specific organic compound classes using a series of sequential chemical extractions; these include TCA (trichloroacetic acid), hot dilute acid treatment, charcoal and organic solvent extraction. The fractions originally defined by Miyata & Hattori are: Acid-soluble P, Nucleotide P, Sugar P, Acid-soluble Polyphosphate, Orthophosphate, Nucleic Acid P, Acid-insoluble polyphosphate and Lipid P. However, after a thorough testing of the method using extractions of known compounds, DuBois (2008) condensed and redefined the eight fractions into five: Acid-soluble P (includes: Acid-soluble P, Nucleotide P, Sugar P and Orthophosphate), Nucleotide-free acid-soluble P, Acid-soluble polyphosphate, Lipid P and Nucleic Acid P/Acid-insoluble polyphosphate. Acid-soluble P is extracted into solution using cold NaCl and trichloroacetic acid (TCA). Upon neutralization and the addition of activated charcoal, the nucleotide-free acid-soluble P is obtained during step 2. Acid-soluble polyphosphate is extracted using hydrosulfuric acid (H_2SO_4) and heat (100°C). In step 4 the samples are treated with 95% ethyl alcohol and 1:1 ethyl alcohol-ethyl ether to isolate the lipid P. Upon reaching step 5, the samples are again treated with H_2SO_4 and heat (100°C) to obtain the acid insoluble polyphosphate and nucleic acid P. Samples are run in duplicate and standards are matrix-matched to the samples for each step. SRP and TDP are measured at each of the five steps except Step 4 (Lipid P) where only TDP is measured. Measurements for the individual Miyata and Hattori defined fractions (Acid-soluble P, Nucleotide P, Sugar P, Acid-soluble Polyphosphate, Orthophosphate, Nucleic Acid P, Acid-insoluble polyphosphate and

Lipid P) can be found using basic equations that involve the SRP and TDP measurements from the various steps.

3.2.2.1 First two spike trials

Seven P compounds (sodium phosphate, sodium triphosphate, glyphosate, ATP, glycerophosphate, glucose-1-phosphate and potassium pyrophosphate; Table 3.2) were dry spiked into estuarine sediment, mixed to a homogenous consistency and analyzed using the Miyata & Hattori method. 'x' grams of each compound (to yield 95-225 μmol P in each spike) was combined with ~0.04 g estuarine sediment. Each P compound was run in duplicate except for glyphosate in the first trial and glycerophosphate in the second. In these cases, one of the duplicates was lost during processing and results only reflect one of each of these compounds as opposed to two.

3.2.2.2 Third spike trial

A third spike trial was conducted using a different set of phosphorus standards (ATP, DNA, RNA, phytic acid, sodium hexametaphosphate, phosphatidylcholine (lecithin) and a mix of DNA, phytic acid and sodium hexametaphosphate; Table 3.3). The spikes were prepared in the same manner as those in the first two trials, yielding 38-105 μmol P per spike and were run in duplicate.

3.2.2.3 Cariaco sediment trap samples

A selection of Cariaco Basin sediment trap samples from cruises 19-22 was analyzed. Depending on the amount of sample available, ~0.005 to 0.05 g of sample was used. Three of the 13 samples were run in duplicate.

3.3 Results

3.3.1 ^{31}P-NMR: 0.25 M NaOH/0.05 M EDTA

Figures 3.3 and 3.4 show the spectra of the individual P compounds that were spiked directly into 0.25 M NaOH/0.05 M EDTA and run on liquid ^{31}P-NMR. Resulting chemical shifts and peak spectra of each compound matched closely with accepted published values.

3.3.2 ^{31}P-NMR: 0.1 M NaAc (pH 5)/Na dithionite

Of the P compounds spiked into estuarine sediment, extracted and analyzed using liquid ^{31}P-NMR, only four (ATP, DNA, phytic acid and sodium hexametaphosphate) of the six were successful in terms of seeing a signal for the P compound when the extract was run. RNA and lecithin (not shown) had no quantifiable peaks in the extracts, suggesting that this method was unsuccessful in extracting these compounds into the liquid phase from the estuarine sediment. We were able to identify the peaks representing each P compound based on published chemical shifts and comparison to the spectra obtained from spiking the compound directly into the extract. Although the peaks' chemical shifts between the two spectra don't match exactly, likely due to degradation, the values are similar enough to verify the P compound present. These spectra are presented side-by-side in figure 3.5.

3.3.3 Miyata & Hattori: First two spike trials

Percent spike recoveries of the standards were calculated based on the total P added for the first (Table 3.4) and second (Table 3.5) trials. Spike recoveries were low in the first trial run and improved during the second trial while using the same P

compounds. As expected, > 50% of the P came out as Acid Soluble P (nucleotide and sugar P and orthophosphate) across all the spikes, with the remaining P extracted as Acid Soluble Poly P in samples. The percent distributions of each spike across the defined Miyata and Hattori classifications from the second trial run were calculated. The classifications include Acid Soluble P, Acid Soluble Poly P, Nucleic Acid P, Acid Insoluble Poly P and Lipid P. The classification of Acid Soluble P includes: Nucleotide P, Sugar P and Orthophosphate). The data were plotted (Figure 3.6) to gain a visual perspective of the distribution across the classifications for each spike. As the P compounds tested were identical between the two trials and percent recoveries were better during trial two, only the Miyata & Hattori results from the second trial are plotted and presented.

3.3.4 Miyata & Hattori: Third spike trial

Once again, percent spike recoveries of the standards were calculated based on the total P added (Table 3.6). As expected, P was extracted in a wider range of fractions across these spikes due to the more unique P standards used in this trial. Spike recoveries averaged 75% and were slightly lower than those of the second trial (average spike recovery of 83%). The percent distributions of each spike across the Miyata and Hattori classifications were calculated and plotted (Figure 3.7). The dominant classifications differed slightly from the first two spike trials. Instead of Acid Insoluble Poly P, the fifth classification for this trial was Residual P. Otherwise the same classifications appear as they did in the first two trials (Acid Soluble P, Acid Soluble Poly P, Nucleic Acid P and Lipid P). Extracts from some of these samples (n = 12) were also analyzed using liquid ^{31}P-NMR to see if we could verify the results obtained from Miyata & Hattori.

Specifically, we found the spectra of DNA and sodium hexametaphosphate agreed well with the classification distribution determined via Miyata & Hattori (Figures 3.8 and 3.9).

3.3.5 Cariaco sediment trap samples

As done previously with the spike trials, the percent distributions of each of the 13 samples across the Miyata & Hattori classifications were calculated and plotted (Figure 3.10). The dominant classification for these samples was Acid Soluble P (nucleotide and sugar P and orthophosphate), > 40% in all the samples. Residual P was the second largest fraction, accounting for 10-40% of the P. The remaining P in the samples can be attributed to Nucleic Acid P, Acid Insoluble Poly P and Lipid P. The greatest variability across the samples is seen their percentages of Acid Soluble P and Residual P, although between some samples these numbers are comparable.

3.4 Discussion

3.4.1 ^{31}P-NMR: 0.25 M NaOH/0.05 M EDTA

In order to interpret and understand the P spectra, it is useful to understand why spectra appear the way they do. For examples, tripolyphosphate's spectrum shows two peaks, a large one at -5 ppm and a smaller one at -20 ppm (Figure 3.3). This is as expected. The smaller peak is the signal for the middle P in tripolyphosphate, with the larger peak representing the P at either end. It is important to note that the large peak at -5 ppm is representative of pyrophosphate, which is consistent with their location in the tripolyphosphate molecule.

The three different methylphosphonates analyzed were chosen to illustrate ^{31}P-NMR's ability to differentiate P compounds within the same compound class (Figure 3.4). Polyphosphates of different chain lengths were run for a similar reason, to exhibit

the instrument's ability to differentiate between compound lengths, even when each P group is identical to its neighbor. As chain length increases, the polyphosphate peak at -20 ppm grows. Simultaneously, the two peaks at approximately zero and -7 ppm shrink, if not disappear.

3.4.2 ^{31}P-NMR: 0.1 M NaAc (pH 5)/Na dithionite

Phytic acid, DNA, ATP and sodium hexametaphosphate were successfully extracted from estuarine sediment, as evidenced from the comparison between each compound's extracted and direct spike spectra (Figure 3.5). RNA and lecithin were not successfully extracted (spectra not shown), most likely due to the fact that both compounds were very difficult to mix homogenously with the estuarine sediment and dissolve in the extractant.

Phytic acid is a cyclic compound with six phosphate groups that produces a signal at 5 ppm as seen in both the extracted and direct spike spectra. This chemical shift is attributed to orthophosphate which means that the phytic acid most likely broke down into individual phosphate groups when exposed to the extractant. DNA should produce a signal just on the positive side of zero, up to ~1 ppm. This is precisely where the peak is in the spectrum of DNA's direct spike. In comparison to the extracted DNA spectrum, we see a peak at approximately the same location indicating it was indeed extracted from the estuarine sediment. However, there is a larger peak at approximately 5 ppm, which is attributed to orthophosphate that was extracted from the estuarine sediment itself. The three peaks seen in the spectrum of ATP's direct spike represent the three phosphorus groups found in ATP. Each P produces a separate signal because each is unique structurally within the ATP molecule. As with DNA, the extracted ATP spectrum shows

three peaks at the same chemical shifts as those seen in the direct spike spectrum, indicating successful extraction. But once again, there is an extra peak at ~5 ppm due to orthophosphate derived from the estuarine sediment. Finally, in comparing the two sodium hexametaphosphate spectra, we see that they mirror one another in number of peaks and peak locations, thus suggesting it was successfully extracted from the estuarine sediment. The fact that the largest peak is at -20 makes sense as sodium hexametaphosphate is a cyclic polyphosphate. The other smaller peaks at 5 and -5 ppm represent orthophosphate and pyrophosphate, respectively. These are most likely due to some breakdown of sodium hexametaphosphate as well as the orthophosphate associated with the estuarine sediment.

3.4.3 Miyata & Hattori: First two spike trials

Percent recoveries were lower during the first spike trial (Table 3.4) due to unfamiliarity with the method and the need to work out any issues encountered. Recoveries improved for the second trial run (Table 3.5) as the method became more familiar. The second spike trial was done with more care and patience, but also with more confidence and thus better recoveries were obtained.

Six of the seven P compounds tested in the second trial run were extracted as anticipated (Figure 3.6). The majority of sodium phosphate was extracted in the Acid Soluble P fraction, as expected. Just over 60% of the sodium triphosphate was also extracted in the Acid Soluble P fraction, with the remainder appearing in the Acid Soluble Poly P fraction. These results were not unexpected. Sodium triphosphate is a short-chain polyphosphate and is therefore less stable and more susceptible to breakdown during the first acid treatment. The acid can potentially break the O – P bonds and

protonate the phosphate groups. As expected, > 95% of the glyphosate was extracted in the Acid Soluble P fraction. The distribution of ATP across the Acid Soluble P and Acid Soluble Poly P fractions can be explained in the same manner as that of sodium triphosphate, breakdown of the O – P bonds followed by protonation. More than 90% of glycerophosphate was extracted as Acid Soluble P; again, this was expected for this compound's extraction. Potassium pyrophosphate's distribution is expected with two-thirds being extracted as Acid Soluble P; as pyrophosphate is only two phosphate groups, it is not especially stable and can be broken down to individual phosphate groups with relative ease using acid.

The only P compound whose extraction could not be fully explained was glucose-1-phosphate. The compound was distributed evenly between Acid Soluble P and Acid-soluble Poly P. Its extraction into the Acid Soluble P fraction is as expected, given that the compound is a sugar phosphate, another phosphorus type grouped under this fraction. However, the remaining 50% appeared in the Acid Soluble Poly P fraction; this was not expected as this compound only contains one phosphorus and therefore not a polyphosphate. This could potentially be due to the sugar producing a tighter absorption to the estuarine sediment through an oxide association between the sugar's phosphate group and an element in the sediment.

3.4.4 Miyata & Hattori: Third spike trial

The lower average percent in this trial (75%) as compared to the second trial (83%) can most likely be attributed to the type of compounds extracted in the third trial which included RNA and DNA, both of which are insoluble in long chain length form and less likely to dissolve, thereby yielding the lowest recoveries.

All spikes, except RNA, were extracted as expected (Figure 3.7). As with the second trial, ATP was extracted in approximately equal parts Acid Soluble P and Acid Soluble Poly P. ATP is a short polyphosphate and less resistant to breakdown during the first acid treatment. Between the duplicates, ~70% of DNA was extracted as Nucleic Acid P, where we would expect the majority of it to appear. More than 90% of phytic acid came out in the Acid Soluble P fraction as anticipated. Sodium hexametaphosphate's distribution of equal parts Acid Soluble Poly P and Acid Soluble P can be explained by the likelihood that this cyclic structure was broken apart during the first acid treatment, producing both phosphate and polyphosphate groups. The majority of phosphatidylcholine's extraction as Lipid P was also expected as it is a lipid, more commonly known as lecithin. And finally, the mix spike exhibited an extraction distribution that reflects the three P compounds that comprised the spike, DNA (Lipid P fraction), sodium hexametaphosphate (Acid Soluble P and Acid Soluble Poly P fractions) and phytic acid (Acid Soluble P fraction).

Only ~40% of RNA extracted into the Nucleic Acid P fraction (where we would expect it to), with the remaining RNA extracted in equal parts as Acid Soluble P and Residual P (accounting for another 40%) and equal parts Lipid P and Acid Soluble Poly P (accounting for the remaining 20%). This is perhaps as expected though because of RNA's inherent insolubility.

Extracts from the Miyata & Hattori analyses of DNA and hexametaphosphate were run using liquid ^{31}P-NMR. The spectrum of the extracted DNA (Figure 3.8) shows a large sharp peak around -1 ppm, a chemical shift that agrees closely with experimental and published DNA chemical shifts between -0.3 and -0.9. A second small peak is visible

around -10 ppm, which is likely due to breakdown. There are three distinct peaks on the extracted sodium hexametaphosphate spectrum (Figure 3.9). Peaks at 5 and -5 ppm are consistent with mono (12%) and diesters (50%), respectively, both of which are a likely result of the sodium hexametaphosphate break down. The third peak at -20 ppm is indicative of polyphosphates (38%), which is expected since sodium hexametaphosphate is a cyclic polyphosphate. Again, these ^{31}P-NMR results are consistent with this compound's extraction as Acid Soluble P and Acid Soluble Poly P from Miyata & Hattori. The mono- and diester peaks can be equated with Acid Soluble P and the polyphosphate peak with Acid Soluble Poly P. The Miyata & Hattori results agree reasonably well with the ^{31}P-NMR relative peak distributions: 62% from mono- and diester peaks compared to 50% Acid Soluble P and 38% from the polyphosphate peak compared to 50% Acid Soluble Poly P.

3.4.5 Cariaco sediment trap samples

Acid Soluble P and Residual P are the largest fractions in all the samples (3.10). Based upon the fact that this is an organic fractionation method, we believe all the fractions we see are attributable to organic P except the Residual P which could be from any PIP that was leached from the sample during the process. However, this could very well be an underestimation of the amount of PIP that came from the sample during the fractionation as some of it could have come out in the Acid Soluble P fraction as well. By combining the SEDEX data we have on these samples (which breaks down the PIP and gives us a value for the POP fraction as a whole) with the results from Miyata & Hattori, we can make conservative estimates of what components make up the POP pool (a value determined using SEDEX).

According to the SEDEX results of these samples, on average, POP comprises 40±8% of the TPP pool, followed by labile (25±16%) and oxide bound (26±14%) P accounting for approximately equal parts P. Authigenic and detrital P contribute the least to the TPP pool at 6±5% and 2±1%, respectively. The 40% POP can be further broken down using the Miyata & Hattori results. On average, Acid Soluble P dominates the POP fraction (58±13%) indicating ~60% of the POP is comprised of orthophosphate, nucleotides and sugar P. Nucleic acid and lipid P and polyphosphates contribute much smaller percentages (2-6% each) to POP. The remaining P measured using Miyata & Hattori is attributed to Residual P (28±10%), which, as previously mentioned, we believe is PIP that was leached from the samples during the method. In contrast to our findings of POP composition in sediment trap samples, Miyata & Hattori (1986) found orthophosphate and nucleic acids to be the most abundant types of P in phytoplankton, followed by polyphosphates and lipids.

3.5 Conclusions

We've shown that the Miyata & Hattori method and liquid ^{31}P-NMR spectroscopy are valuable tools for distinguishing and identifying different kinds of POP. Spike trials demonstrate Miyata & Hattori's ability to extract and isolate P compounds in the fractions expected. This application to actual sediment trap samples also demonstrates its 'real life' application and usefulness. It is exciting to see that not only can PIP be broken down in sediment trap samples, but POP as well, using the Miyata & Hattori method. We also saw the value of using this method in conjunction with liquid ^{31}P-NMR on P-spiked samples. ^{31}P-NMR was able to verify our Miyata & Hattori results for the presence of two P compounds, DNA and sodium hexametaphosphate, in the fractions we

expected for each. Relative to the large amount of Cariaco sediment trap samples we have available to us, only a handful were analyzed using the Miyata & Hattori method, but with promising results. We could obtain very interesting results were more sediment trap samples run using this method and only due to time constraints and the time intensiveness of the method were not more run for this thesis.

Table 3.1 Chemical shift ranges (ppm) of P compounds and classes in ^{31}P-NMR.

P Class	P Compound	Chemical Shift (ppm)
Phosphonate		30 to 15
	Methylphosphonate	30 to 25
	2-aminoethylphosphonic acid (AEP)	~20
	Glyphosate	~17
Phosphate monoester		8 to 0
	Glucose-6-phosphate	5.5 to 3.5
Orthophosphate		5 to 0
	Glycerophosphate	5.5 to 4.5
Nucleic Acids		0.5 to -1
	RNA	0.5
	DNA	-0.3 to -0.9
Phosphate diester		0 to -5
Pyrophosphate		-5 to -10
	Potassium diphosphate	-5 to -5.5
Polyphosphate		-18 to -30
	Large polyphosphate chains	-22

Table 3.2 P compounds used in the first two spike trial runs of Miyata & Hattori, their abbreviations and their compound type.

Common Name	Abbreviation	Compound Type
Sodium Phosphate	P	Orthophosphate
Sodium Triphosphate	T	Polyphosphate
Glyphosate	G	Phosphonate
Adenosine triphosphate (ATP)	A	Nucleotide
Glycerophosphate	GP	Monoester
Glucose-1-phosphate	G1P	Cyclical sugar phosphate
Potassium pyrophosphate	PP	Pyrophosphate

Table 3.3 P compounds used in the third spike trial run of Miyata & Hattori, their abbreviations and their compound type.

Common Name	Abbreviation	Compound Type
Adenosine 5-triphosphate	ATP	Nucleotide
Deoxyribonucleic Acid	DNA	Nucleic Acid
Ribonucleic Acid	RNA	Nucleic Acid
Phytic Acid	PhyAc	Cyclic with 6 PO_4 groups
Sodium Hexametaphosphate	NaHex	Cyclic Polyphosphate
Phosphatidylcholine (Lecithin)	Lec	Lipid
Mix (DNA, PhyAc, NaHex)	Mix	See above

Table 3.4 Percent spike recoveries for the first Miyata &Hattori spike trial.

	µmol P/g extracted	calculated µmol P/g added	Total % recovery	Average % recovery ± S.D.
ES + Psp1	704	2348	30	35 ± 6
ES + Psp2	1077	2756	39	
ES + Tsp1	1581	2866	55	46 ± 13
ES + Tsp2	1147	3169	36	
ES + Gsp1	1284	2601	49	
ES + Asp1	1035	2380	43	42 ± 2
ES + Asp2	1002	2486	40	
ES + GPsp1	729	2059	35	33 ± 4
ES + GPsp2	692	2298	30	
ES + G1Psp1	613	1828	34	33 ± 1
ES + G1Psp2	692	2147	32	
ES + PPsp1	1265	2636	48	55 ± 10
ES + PPsp2	1406	2264	62	

Table 3.5 Percent spike recoveries for the second Miyata & Hattori spike trial.

	µmol P/g extracted	calculated µmol P/g added	Total % recovery	Average % recovery ± S.D.
ES + Psp1	1890	1875	101	90 ± 15
ES + Psp2	1738	2179	80	
ES + Tsp1	1726	1891	91	88 ± 4
ES + Tsp2	1667	1952	85	
ES + Gsp1	959	1710	56	73 ± 24
ES + Gsp2	1518	1699	89	
ES + Asp1	1734	1802	96	91 ± 8
ES + Asp2	1444	1699	85	
ES + GPsp2	1146	1676	68	
ES + G1Psp1	1037	1514	68	59 ± 1
ES + G1Psp2	1083	1544	70	
ES + PPsp1	1833	1902	96	91 ± 7
ES + PPsp2	1549	1796	86	

Table 3.6 Percent spike recoveries for the third Miyata & Hattori spike trial.

	µmol P/g extracted	calculated µmol P/g added	Total % recovery	Average % recovery ± S.D.
ES + ATP_1	1325	1698	78	79 ± 1
ES + ATP_2	1392	1741	80	
ES + DNA_1	899	1268	71	65 ± 8
ES + DNA_2	752	1264	59	
ES + RNA_1	865	1353	64	64 ± 0
ES + RNA_2	857	1353	63	
ES + PhyAC_1	1276	1951	65	65 ± 0
ES + PhyAC_2	1260	1946	65	
ES + NaHex_1	1777	2025	88	92 ± 6
ES + NaHex_2	1928	2005	96	
ES + Lec_1	495	582	85	91 ± 8
ES + Lec_2	423	438	97	
ES + Mix_1	1972	2967	66	68 ± 2
ES + Mix_2	2076	2984	70	

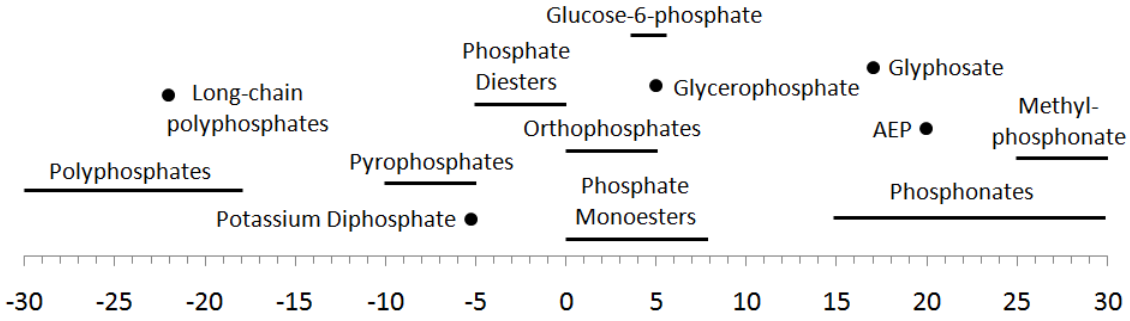

Figure 3.1 Chemical shift ranges (ppm) of P compounds and classes in ^{31}P-NMR.

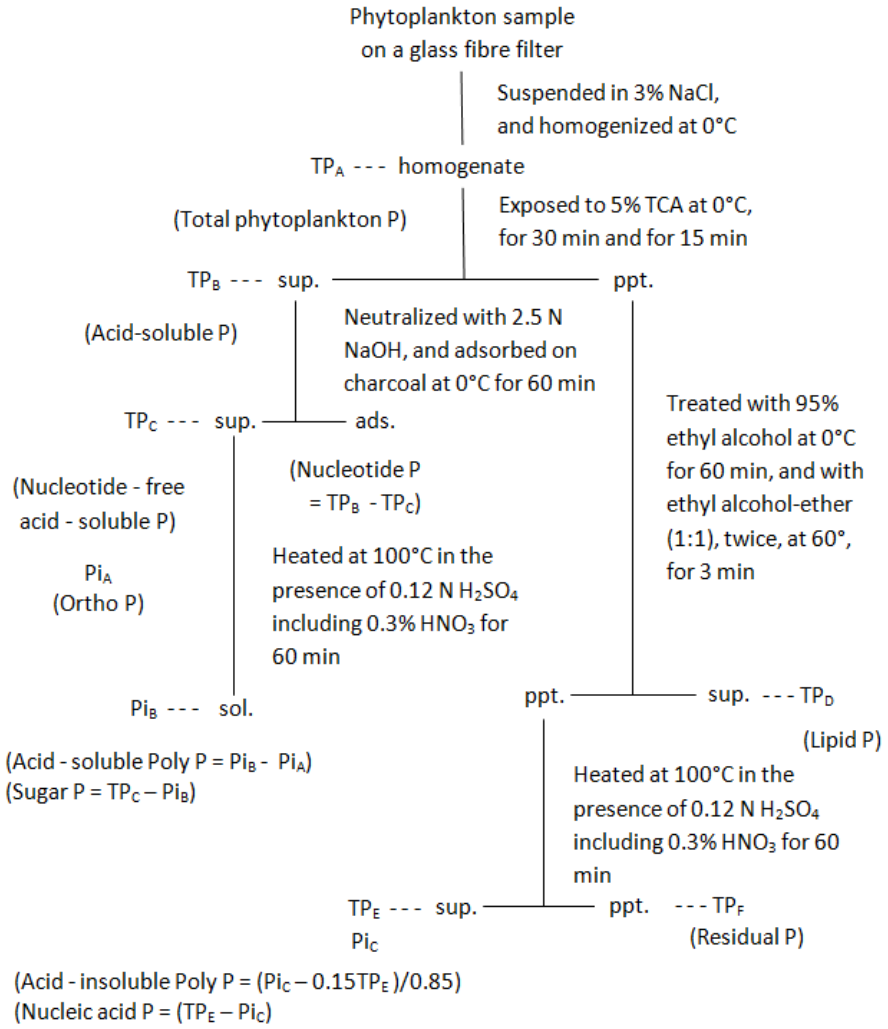

Figure 3.2 A flowchart depicting the steps and experimental conditions of the Miyata & Hattori method.

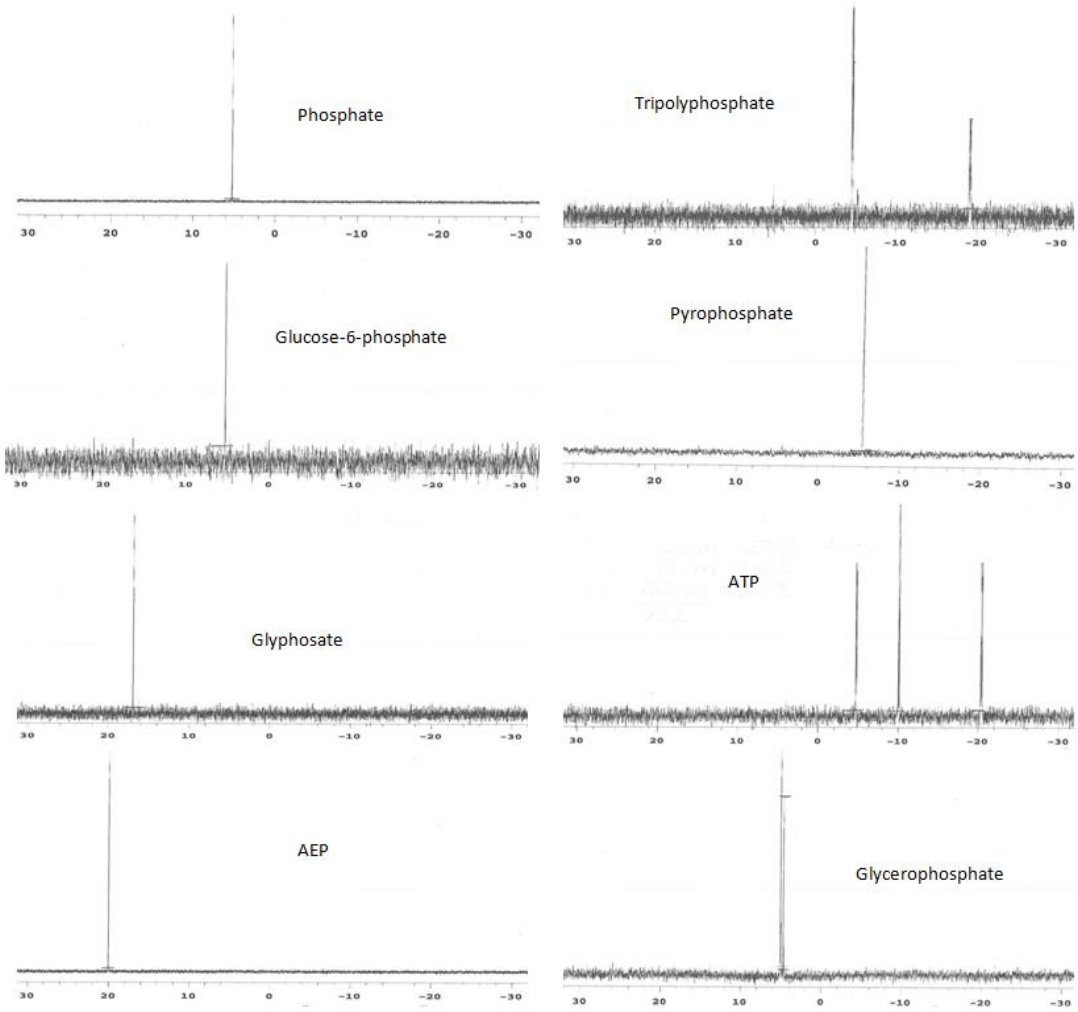

Figure 3.3 Liquid ^{31}P-NMR spectra of P standards spiked directly into 0.25 M NaOH/0.05 M EDTA matrix. ATP = Adenosine triphosphate; AEP = 2-Aminoethylphosphoric acid.

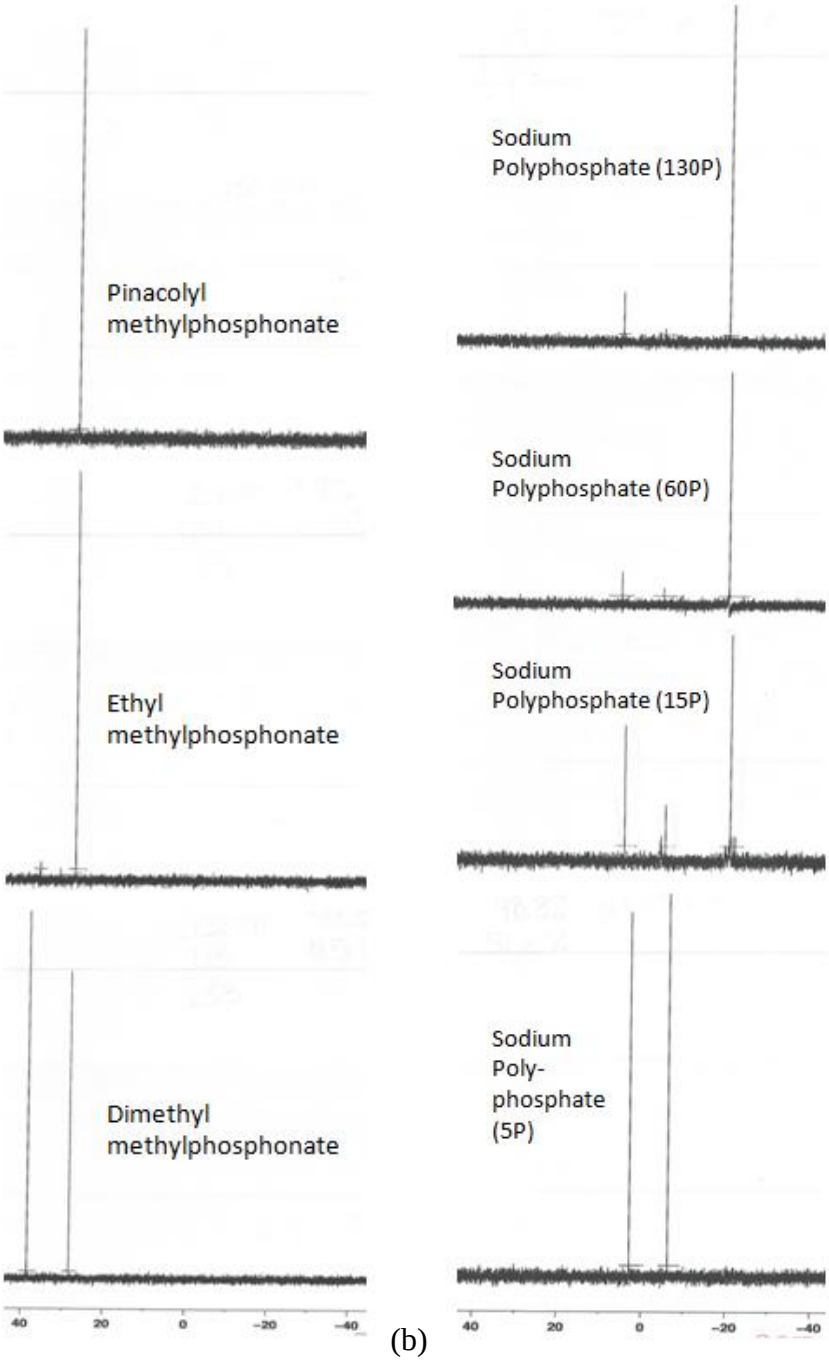

Figure 3.4 Liquid ^{31}P-NMR spectra of (a) methylphosphonate standards and (b) sodium polyphosphates (the number of P in parentheses denotes the number of phosphate groups within the chain) spiked directly into 0.25 M NaOH/0.05 M EDTA matrix.

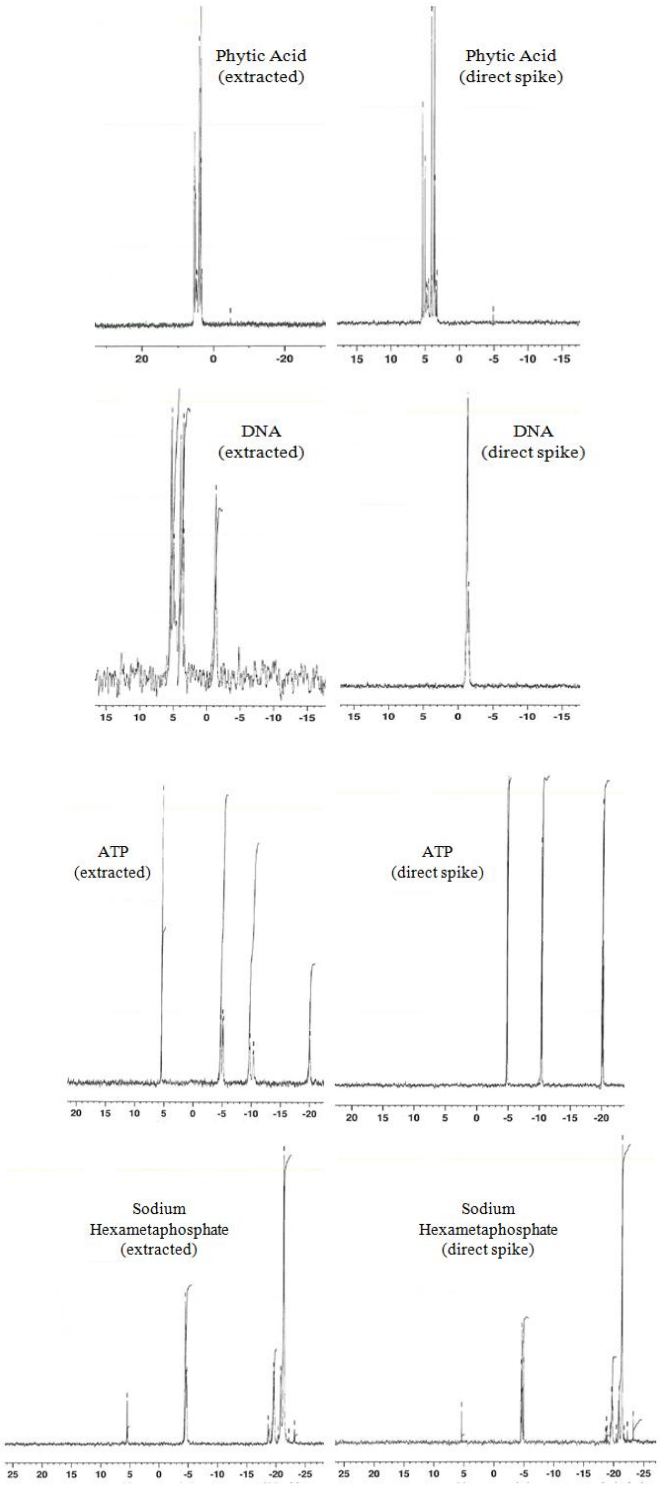

Figure 3.5 Liquid ^{31}P-NMR spectra of P standards extracted from estuarine sediment using 0.1 M NaAc (pH 5)/Na dithionite (left) and of P standards spiked directly into 0.1 M NaAc (pH 5)/Na dithionite (right).

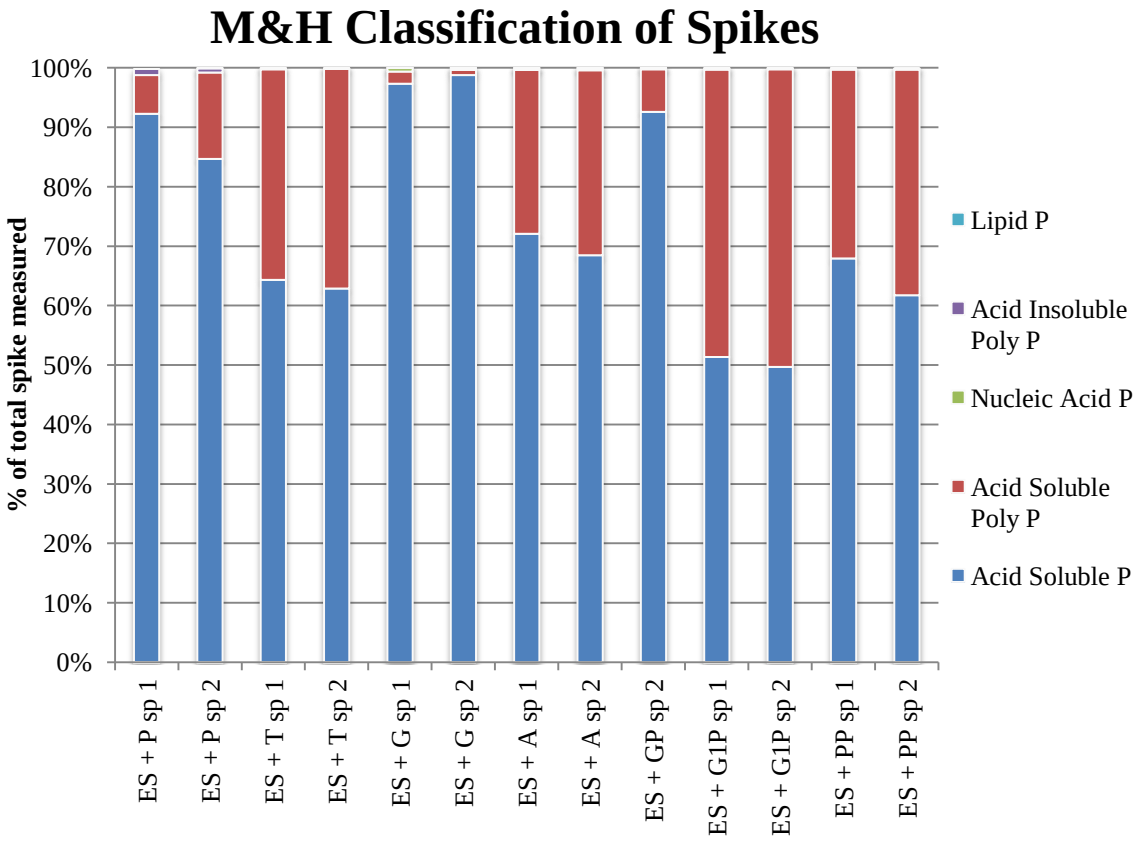

Figure 3.6 Distribution of each spike used in the second trial run over the Miyata & Hattori classifications: Acid Soluble P, Acid Soluble Poly P, Nucleic Acid P, Acid Insoluble Poly P and Lipid P. The classification of Acid Soluble P includes: Nucleotide P, Sugar P and Orthophosphate.

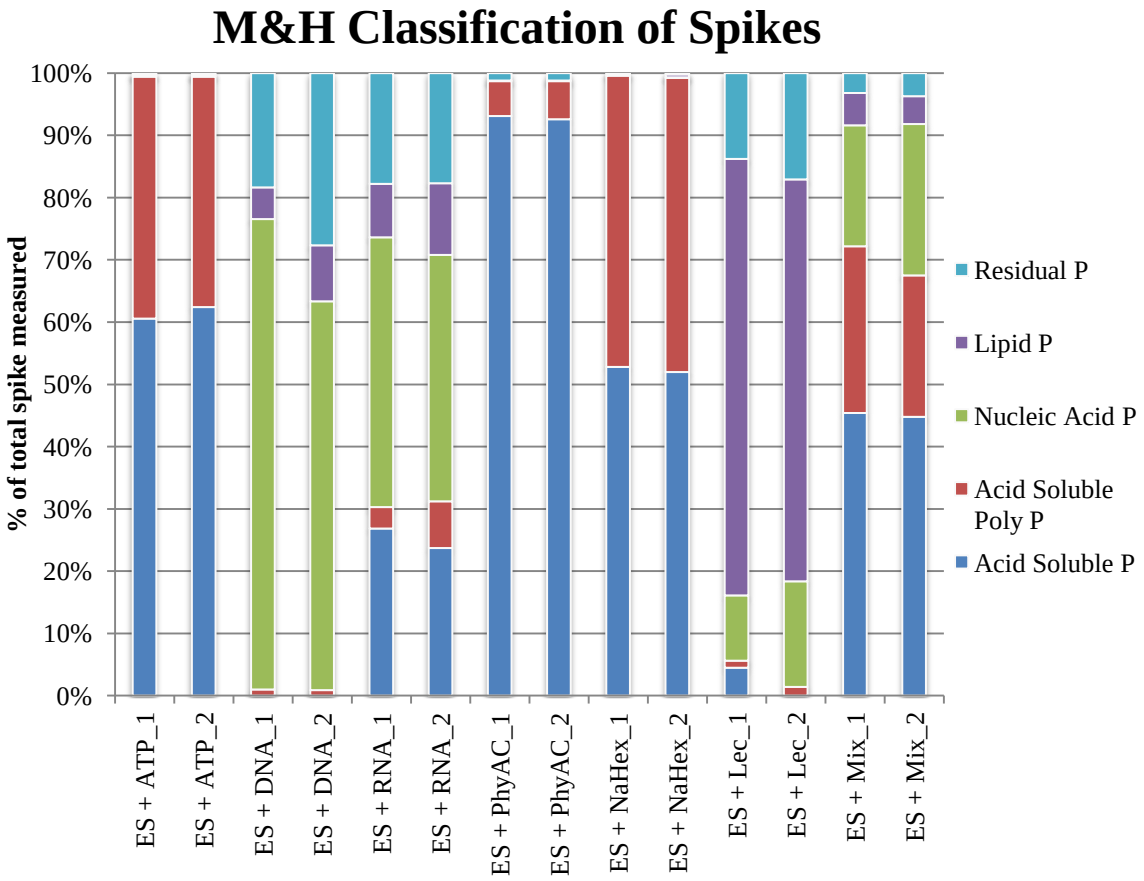

Figure 3.7 Distribution of each spike used in the third trial run over the Miyata & Hattori classifications: Acid Soluble P, Acid Soluble Poly P, Nucleic Acid P, Lipid P and Residual P. The classification of Acid Soluble P includes: Nucleotide P, Sugar P and Orthophosphate.

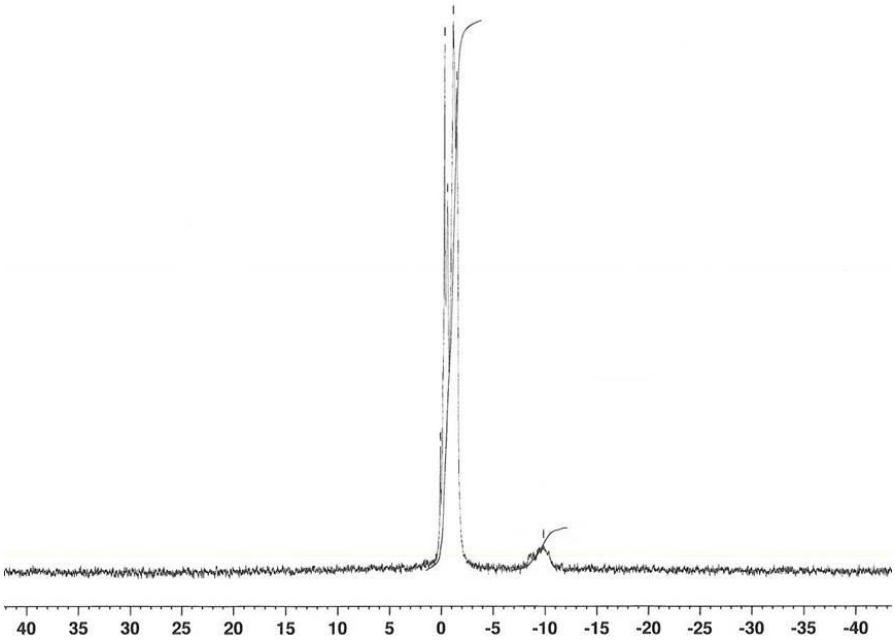

Figure 3.8 Liquid ^{31}P-NMR spectrum of a DNA spike (from the third trial run) that was extracted using the Miyata & Hattori method.

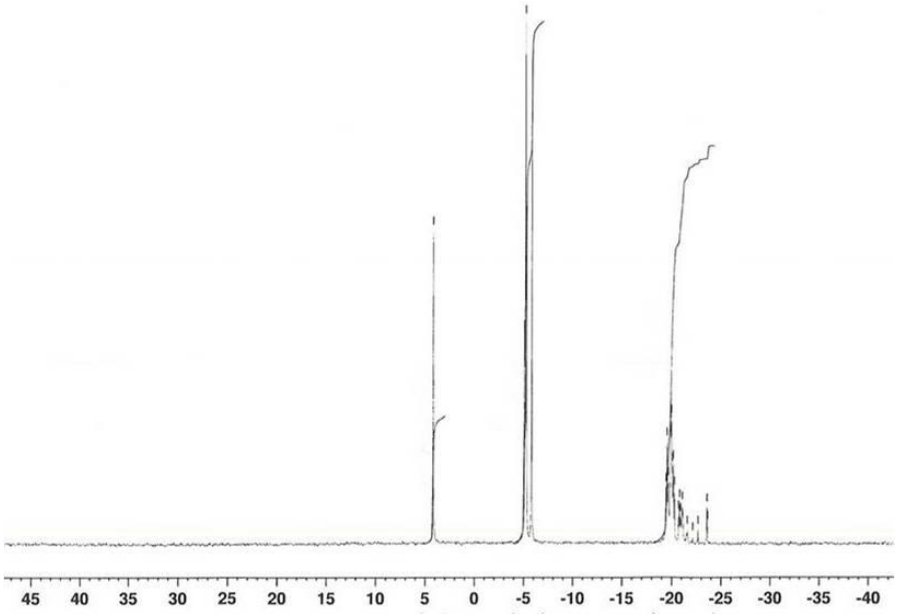

Figure 3.9 Liquid ^{31}P-NMR spectrum of a sodium hexametaphosphate Spike (from the third trial run) that was extracted using the Miyata & Hattori method.

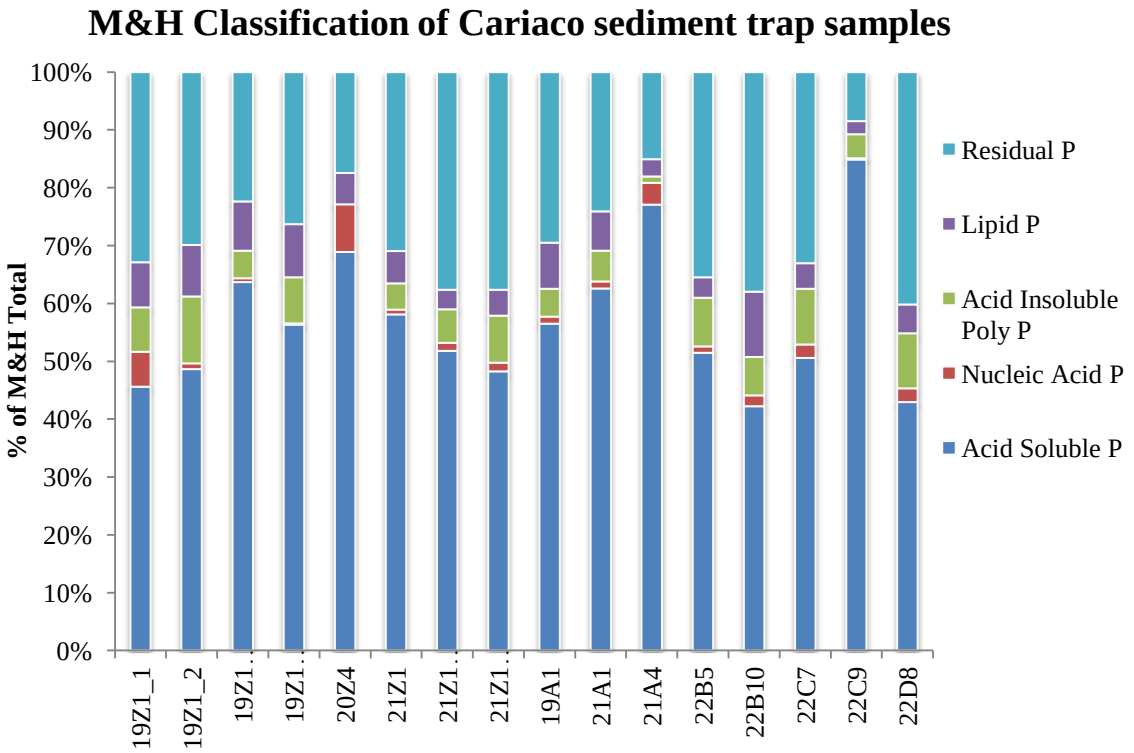

Figure 3.10 Distribution of each selected Cariaco sediment trap sample (from cruises 19-22) over the Miyata & Hattori classifications: Acid Soluble P, Nucleic Acid P, Acid Insoluble Poly P, Lipid P and Residual P. The classification of Acid Soluble P includes: Nucleotide P and Orthophosphate.

REFERENCES

Ammerman, J.W. and F. Azam. 1985. Bacterial 5'-nucleotidase in aquatic ecosystems: a novel mechanism of phosphorus regeneration. *Science*, 227: 1338-1340.

Ammerman, J.W. and F. Azam. 1991a. Bacterial 5'-nucleotidase activity in estuarine and coastal marine waters: characterization of enzyme activity. *Limnology and Oceanography*, 36(7): 1427-1436.

Ammerman, J.W. and F. Azam. 1991b. Bacterial 5'-nucleotidase activity in estuarine and coastal marine waters: role in phosphorus regeneration. *Limnology and Oceanography*, 36(7): 1437-1447.

Anderson, L.D. and M.L. Delaney. 2000. Sequential extraction and analysis of phosphorus in marine sediments: streamlining of the SEDEX procedure. *Limnology and Oceanography*, 45(2): 509-515.

Aspila, K.I., H. Agemian and A.S. Chau. 1976. A semi-automated method for the determination of inorganic, organic and total phosphate in sediments. *Analyst*, 101: 187-197.

Astor, Y., F. Muller-Karger and M.I. Scranton. 2003. Seasonal and interannual variation in the hydrography of the Cariaco Basin: implications for basin ventilation. *Continental Shelf Research*, 23(1): 125-144.

Astor, Y.M., L. Lorenzoni and M. Scranton (Eds.). 2011. Cariaco Time Series Study: Handbook of Methods for the Analysis of Oceanographic Parameters at the Cariaco Time-Series Station.

Beauchemin, S., D. Hesterberg, J. Chou, M. Beauchemin, R.R. Simard and D.E. Sayers. 2003. Speciation of phosphorus in phosphorus-enriched agricultural soils using X-ray absorption near-edge structure spectroscopy and chemical fractionation. *Journal of Environmental Quality*, 32(5): 1809-1819.

Benitez-Nelson, C.R. 2000. The biogeochemical cycling of phosphorus in marine systems. *Earth-Science Reviews*, 52: 109-135.

Benitez-Nelson, C.R., L. O'Neill, L.C. Kolowith, P. Pellechia and R. Thunell. 2004. Phosphonates and particulate organic phosphorus cycling in an anoxic marine basin. *Limnology and Oceanography*, 49(5): 1593-1604.

Benitez-Nelson, C.R., L.P. O'Neill Madden, R.M. Styles, R.C. Thunell and Y. Astor. 2007. Inorganic and organic sinking particulate phosphorus fluxes across the oxic/anoxic water column of Cariaco Basin, Venezuela. *Marine Chemistry,* 105: 90-100.

Benitez-Nelson, C.R. 2012. Phosphorus biogeochemistry, what have we learned and where do we need to go in the future? Presentation, Gordon Research Conference.

Cade-Menun, B.J. and C.M. Preston. 1996. A comparison of soil extraction procedures for ^{31}P NMR spectroscopy. *Soil Science,* 161(11): 770-785.

Cade-Menun, B.J., C.R. Benitez-Nelson, P. Pellechia and A. Paytan. 2005. Refining ^{31}P nuclear magnetic resonance spectroscopy for marine particulate samples: storage conditions and extraction recovery. *Marine Chemistry,* 97: 293-306.

Cade-Menun, B.J. and A. Paytan. 2010. Nutrient temperature and light stress alter phosphorus and carbon forms in culture-grown algae. *Marine Chemistry,* 121: 27-36.

Carman, R., G. Edlund and C. Damberg. 2000. Distribution of organic and inorganic phosphorus compounds in marine and lacustrine sediments: a ^{31}P NMR study. *Chemical Geology,* 163: 101-114.

Clark, L.L., E.D. Ingall and R. Benner. 1998. Marine phosphorus is selectively remineralized. *Nature,* 393: 426.

Clark, L.L., E.D. Ingall and R. Benner. 1999. Marine organic phosphorus cycling: novel insights from nuclear magnetic resonance. *American Journal of Science,* 299: 724-737.

Delaney, M.L. 1998. Phosphorus accumulation in marine sediments and the oceanic phosphorus cycle. *Global Biogeochemical Cycles,* 12(4): 563-572.

Diaz, J., E. Ingall, C. Benitez-Nelson, D. Paterson, M.D. de Jonge, I. McNulty and J.A. Brandes. 2008. Marine polyphosphate: a key player in geologic phosphorus sequestration. *Science,* 320(5876): 652-655.

Diaz, J.M. and E.D. Ingall. 2010. Fluorometric quantification of natural inorganic polyphosphate. *Environmental Science & Technology*, 44(12): 4665-4671.

DuBois, S. 2008. Characterization of inorganic and organic phosphorus species in particulate matter in the San Pedro Basin, California. M.S. thesis, University of South Carolina.

Dyhrman, S.T., P.D. Chappell, S.T. Hay, J.W. Moffett, E.D. Orchard, J.B. Waterbury and E.A. Webb. 2006. Phosphonate utilization by the globally important marine diazotroph *Trichodesmium*. *Nature,* 439: 68-71.

Dyhrman, S., J. Ammerman and B. Van Mooy. 2007. Microbes and the marine phosphorus cycle. *Oceanography*, 20: 110-116.

Dyhrman, S.T., C.R. Benitez-Nelson, E.D. Orchard, S.T. Haley and P.J. Pellechia. 2009. A microbial source of phosphonates in oligotrophic marine systems. *Nature Geoscience*, 639: 1-4.

Faul, K.L., A. Paytan and M.L. Delaney. 2005. Phosphorus distribution in sinking oceanic particulate matter. *Marine Chemistry,* 97: 307-333.

Froelich, P.N., M.L. Bender and N.A. Luedtke. 1982. The marine phosphorus cycle. *American Journal of Science,* 282: 474-511.

Goñi, M., H.L. Aceves, R.C. Thunell, E. Tappa, D. Black, Y. Astor, R. Varela and F. Muller-Karger. 2003. Biogenic fluxes in the Cariaco Basin: a combined study of sinking particulates and underlying sediments. *Deep-Sea Research Part I*, 50(6): 781-807.

Haberer, J.L. and J.A. Brandes. 2003. A high sensitivity, low volume HPLC method to determine soluble reactive phosphate in freshwater and saltwater. *Marine Chemistry*, 82(3-4): 185-196.

Hannides, C.S., M.R. Landry, C.R. Benitez-Nelson, R.M. Styles, J.P. Montoya and D.M. Karl. 2009. Export stoichiometry and migrant-mediated flux of phosphorus in the North Pacific Subtropical Gyre. *Deep-Sea Research Part I*, 56: 73-88.

He, Z., W. Honeycutt, T.S. Griffin, B.J. Cade-Menun, P.J. Pellechia and Z. Dou. 2009. Phosphorus forms in conventional and organic dairy manure identified by solution and solid state P-31 NMR spectroscopy. *Journal of Environmental Quality,* 38: 1909-1918.

Hebel, D.V. and D.M. Karl. 2001. Seasonal, interannual and decadal variations in particulate matter concentrations and composition in the subtropical North Pacific Ocean. *Deep-Sea Research Part II,* 48: 1669-1695.

Hecky, R.E. and P. Kilham. 1988. Nutrient limitation of phytoplankton in freshwater and marine environments: a review of recent evidence on the effects of enrichment. *Limnology and Oceanography*, 33(4, part 2): 796-822.

Holmes, D. 2004. Basic NMR concepts: a guide for the modern laboratory. Michigan State University.

Karl, D.M. and K. Björkman. 2002. Dynamics of DOP. In: Hansell, D. and C. Carlson (Eds.), *Biochemistry of marine dissolved organic matter*. Elsevier, USA, 246-366.

Karl, D.M., L. Beversdorf, K.M. Björkman, M.J. Church, A. Martinez and E.F. DeLong. 2008. Aerobic production of methane in the sea. *Nature Geoscience*, 1: 473-478.

Karl, D.M. 2014. Microbially mediated transformations of phosphorus in the sea: new views of an old cycle. *Annual Review of Marine Science*, 6: 279-337.

Kelly, A. 2013. Measuring particulate phosphorus: a comparison of two methods. Poster, REU.

Kolowith, L.C., E.D. Ingall and R. Benner. 2001. Composition and cycling of marine organic phosphorus. *Limnology and Oceanography*, 46(2): 309-320.

Koroleff, F. 1983. Determination of nutrients. In: Grasshoff, K., Ehrherd, M. and Kremling, K. (Eds.), *Methods of Seawater Analysis*. Verlag Chemie, Weinheim, 125-135.

Lampert, W. 1978. Release of dissolved organic carbon by grazing phytoplankton. *Limnology and Oceanography*, 23(4): 831-834.

Loh, A.N. and J.E. Bauer. 2000. Distribution, partitioning and fluxes of dissolved and particulate organic C, N and P in the eastern North Pacific and Southern Oceans. *Deep-Sea Research Part I*, 47: 2287-2316.

Lomas, M.W., A.L. Burke, D.A. Lomas, D.W. Bell, C. Shen, S.T. Dyhrman and J.W. Ammerman. 2010. Sargasso Sea phosphorus biogeochemistry: an important role for dissolved organic phosphorus (DOP). *Biogeosciences*, 7: 695-710.

Lomas, M.W., N.R. Bates, R.J. Johnson, A.H. Knap, D.K. Steinberg and C.A. Carlson. 2013. Two decades and counting: 24-years of sustained open ocean biogeochemical measurements in the Sargasso Sea. *Deep-Sea Research II*, 93: 16-32.

Longhurst, A.R. 1991. Role of the marine biosphere in the global carbon cycle. *Limnology and Oceanography*, 36(8): 1507-1526.

Lorenzoni, L., R.C. Thunell, C.R. Benitez-Nelson, D. Hollander, N. Martinez, E. Tapp, R. Varela, Y. Astor and F.E. Müller-Karger. 2009. The importance of subsurface nepheloid layers in transport and delivery of sediments to the eastern Cariaco Basin, Venezuela. *Deep-Sea Research I*, 56: 2249-2262.

Lyons, G., C.R. Benitez-Nelson and R.C. Thunell. 2011. Phosphorus composition of sinking particles in the Guaymas Basin, Gulf of California. *Limnology and Oceaongraphy*, 56(3): 1093-1105.

Mahowald, N., T.D. Jickells, A.R. Baker, P. Artaxo, C.R. Benitez-Nelson, G. Bergametti, T.C. Bond, Y. Chen, D.D. Cohen, B. Herut, N. Kubilay, R. Losno, C. Luo, W. Maenhaut, K.A. McGee, G.S. Okin, R.L. Siefert and S. Tsukuda. 2008. Global distribution of atmospheric phosphorus sources, concentrations and deposition rates, and anthropogenic inputs. *Global Biogeochemical Cycles*, 22: GB4026

Martinez, N.C., R.W. Murray, R.C. Thunell, L.C. Peterson, F. Müller-Karger, Y. Astor and R. Varela. 2007. Modern climate forcing of terrigenous deposition in the tropics (Cariaco Basin, Venezuela). *Earth and Planetary Science Letters*, 254: 438-451.

Martiny, A.C., C.T.A. Pham, F.W. Primeau, J.A. Vrugt, J.K. Moore, S.A. Levin and M.W. Lomas. 2013. Strong latitudinal patterns in the elemental ratios of marine plankton and organic matter. *Nature Geoscience*, 1757: 1-5.

Miyata, K. and A. Hattori. 1986. A simple fractionation method for determination of phosphorus components in phytoplankton: application to natural populations of phytoplankton in summer surface waters of Tokyo Bay. *Journal of the Oceanographical Society of Japan*, 42: 255-265.

Müller-Karger, F., R. Varela, R. Thunell, M. Scranton, R. Bohrer, G. Taylor, J. Capelo, Y. Astor, E. Tappa, T.Y. Ho, M. Iabichella, J.J. Walsh and J.R. Diaz. 2000. Sediment record linked to surface processes in the Cariaco Basin. Eos, Transactions, *American Geophysical Union*, 81(45): 529, 534-535.

Müller-Karger, F., R. Varela, R. Thunell, M. Scranton, R. Bohrer, G. Taylor, J. Capelo, Y. Astor, E. Tappa, T.Y. Ho and J.J. Walsh. 2001. Annual cycle of primary production in the Cariaco Basin: response to upwelling and implications for vertical export. *Journal of Geophysical Research-Oceans*, 106(C3): 4527-4542.

O'Neill, L.P., C.R. Benitez-Nelson, R.M. Styles, E. Tappa and R.C. Thunell. 2005. Diagenetic effects on particulate phosphorus samples collected using formalin poisoned sediment traps. *Limnology and Oceanography-Methods*, 3: 308-317.

Orchard, E.D., C.R. Benitez-Nelson, P.J. Pellechia, M.W. Lomas and S.T. Dyhrman. 2010. Polyphosphate in *Trichodesmium* from the low-phosphorus Sargasso Sea. *Limnology and Oceanography*, 55(5): 2161-2169.

Paytan, A., B.J. Cade-Menun, K. McLaughlin and K.L. Faul. 2003. Selective phosphorus regeneration of sinking marine particles: evidence from ^{31}P-NMR. *Marine Chemistry*, 82: 55-70.

Paytan, A. and K. McLaughlin. 2007. The oceanic phosphorus cycle. *Chemical Reviews*, 107: 563-576.

Peterson, L.C. and G.H. Haug. 2006. Variability in the mean latitude of the Atlantic Intertropical Convergence Zone as recorded by riverine input of sediments to the Cariaco Basin. *Palaeoceanography, Palaeoclimatology, Palaeoecology*, 234:97-113.

Redfield, A.C. 1958. The biological control of chemical factors in the environment. *American Scientist*, 46(3): 205-221.

Redfield, A.C., B.H. Ketchum and F.A. Richards. 1963. The influence of organisms on the composition of seawater. In: Hill, M.N. (Ed.), *The Sea*. Interscience, 26-77.

Ranhofer, M.L., E. Lawrenz, J.L. Pinckney, C.R. Benitez-Nelson and T.L. Richardson. 2009. Cell-specific alkaline phosphatase expression by phytoplankton in Winyah Bay, South Carolina, USA. *Estuaries Coasts*, 32(5): 943-957.

Ruttenberg, K.C. 1992. Development of a sequential extraction method for different forms of phosphorus in marine sediments. *Limnology and Oceanography*, 37(7): 1460-1482.

Ruttenberg, K.C. 2003. The global phosphorus cycle. In: Schlesinger, W.H., Holland, H.D. and Turekian, K.K. (Eds), *Treatise on Geochemistry, Volume 8*. Elsevier, USA, 585-643.

Sannigrahi, P. 2005. Nuclear magnetic resonance spectroscopy: overview of methodology and applications to natural organic matter. PhD dissertation, Georgia Institute of Technology.

Sannigrahi, P. and E. Ingall. 2005. Polyphosphates as a source of enhanced P fluxes in marine sediments overlain by anoxic waters: evidence from ^{31}P NMR. *Geochemical Transactions*, 6(3): 52-59.

Sannigrahi, P., E.D. Ingall and R. Benner. 2006. Nature and dynamics of phosphorus-containing components of marine dissolved and particulate organic matter. *Geochimica Et Cosmochimica Acta*, 70(23): 5868-5882.

Scranton, M., G. Taylor, Y. Astor and F. Müller-Karger. 2006. Temporal variability in the nutrient chemistry of the Cariaco Basin. In: Neretin, L.N. (Ed.), *Past and Present Marine Water Column Anoxia. NATO Science Series: IV: Earth and Environmental Sciences, Volume 64*. Spring, Netherlands, 139-160.

Sekula-Wood, E., C.R. Benitez-Nelson, M.A. Bennett and R. Thunell. 2012. Magnitude and composition of sinking particulate phosphorus fluxes in Santa Barbara Basin, California. *Global Biogeochemical Cycles*, 26(GB2023): 1-15.

Suzumura, M. and E.D. Ingall. 2004. Distribution and dynamics of various forms of phosphorus in seawater: insights from field observations in the Pacific Ocean and a laboratory experiment. *Deep-Sea Research Part I*, 51: 1113-1130.

Taylor, G.T., M. Iabichella, T. Ho, M.I. Scranton, R.C. Thunell, F. Muller-Karger and R. Varela. 2001. Chemoautotrophy in the redox transition zone of the Cariaco Basin: a significant midwater source of organic carbon production. *Limnology and Oceanography*, 46(1): 148-163.

Taylor, G.T., F. E. Muller-Karger, R.C. Thunell, M.I. Scranton, Y. Astor, R. Varela, L.T. Ghinaglia, L. Lorenzoni, K.A. Fanning, S. Hameed and O. Doherty. 2012. Ecosystem responses in the southern Caribbean Sea to global climate change. *PNAS*, 109(47): 19315-19320.

Thunell, R.C. 1998. Particle fluxes in a coastal upwelling zone: sediment trap results from Santa Barbara Basin, California. *Deep-Sea Research Part II*, 45(8-9): 1863-1884.

Thunell, R., E. Tapp, R. Varela, M. Llano, Y. Astor, F. Muller-Karger and R. Bohrer. 1999. Increased marine sediment suspension and fluxes following an earthquake. *Nature*, 398: 233-236.

Thunell, R.C., R. Varela, M. Llano, J. Collister, F. Muller-Karger and R. Bohrer. 2000. Organic carbon fluxes, degradation, and accumulation in an anoxic basin: sediment trap results from the Cariaco Basin. *Limnology and Oceanography*, 45(2): 300-308.

Twyman, R.M. 2005. Phosphorus-31. In: Worsfold, P., A. Townshend and C. Poole (Eds), *Encyclopedia of Analytical Science (2nd edition.), Volume 6*. Elsevier Science, London, UK, 278-286.

Wallman, K. 2010. Phosphorus imbalance in the global ocean? *Global Biogeochemical Cycles*, 24: GB4030.

White, A.E., D.M. Karl, K.M. Björkman, L.J. Beversdorf and R.M. Letelier. 2010. Production of organic matter by Trichodesmium IMS101 as a function of phosphorus source. *Limnology and Oceanography*, 55(4): 1755-1767.

Wilson, S.E., D.K. Steinberg and K.O. Buesseler. 2008. Changes in fecal pellet characteristics with depth as indicators of zooplankton repackaging of particles in the mesopelagic zone of the subtropical and subarctic North Pacific Ocean. *Deep-Sea Research Part II*, 55(14-15): 1636-1647.

Yoshimura, T., J. Nishioka, H. Saito, S. Takeda, A. Tsuda and M.L. Wells. 2007. Distributions of particulate and dissolved organic and inorganic phosphorus in North Pacific surface waters. *Marine Chemistry*, 103: 112-121.

Young, C.L. and E.D. Ingall. 2010. Marine dissolved organic phosphorus composition: insights from samples recovered using combined electrodialysis/reverse osmosis. *Aquatic Geochemistry*, 16(4): 563-574.

www.bruker.com/en/products/mr/nmr/probes/cryoprobes.html